

EXPERIMENTAL SETUP FOR MEASURING THE MAGNETO-OPTICAL KERR
EFFECT UNDER HIGH ISOTROPIC PRESSURE

THESIS

Presented to the Graduate Council of
Southwest Texas State University

In Partial Fulfillment of
The Requirements

For the Degree
Master of Science

By

Brian Donehew

San Marcos, Texas

December, 2001

ACKNOWLEDGEMENTS

I would like to begin by thanking Mom, Dad and my two sisters, Julie and Andrea, for their moral, material, and financial support since I began this endeavor many, many years ago. I would also like to thank my friends Steven, Louie, Allen, and Ren for making the experience that much more enjoyable.

I am also thankful for the members of my thesis committee, Dr. Crawford and Dr. Gutierrez, and to all my instructors here at Southwest Texas and at Texas-San Antonio. I would also like to thank Dr. Galloway and Evelyn Mitchell for their help with the chemical mechanical polisher, and Dr. Stan Tozer of the National High Magnetic Field Laboratory for his very helpful suggestions and ideas. Finally, I'd like to thank my faculty advisor, Dr. Geerts, who really should have co-authorship on this thesis.

This manuscript was submitted on December 10, 2001.

Table of Contents

	Page
ACKNOWLEDGEMENTS	iv
LIST OF FIGURES	vii
ABSTRACT	viii
Chapter	
1 INTRODUCTION AND THEORY	1
1.1 Focus of Research	
1.2 Polarization of E-M Waves	
1.3 The Kerr Effect – Macroscopic Description	
1.4 Orientation of the Magnetic Domains	
1.5 The Kerr Effect – Microscopic Description	
1.6 Applications of Magneto-Optical Materials	
2. EXPERIMENTAL SETUP	17
2.1 Setup of the Optical Table for Measuring the Longitudinal Kerr Effect	
2.2 Electronic Setup for Measuring and Analyzing Data	
2.3 The Laser	
2.4 Beam Expander and Focusing Lens	
2.5 Photoelastic Modulator	
2.6 Lock-In Amplifier	
2.7 Theory of Operation	
3. SAPPHIRE BALL CELL	38
3.1 The Diamond Anvil Cell	
3.2 Beryllium Copper Gasket	
3.3 The Sapphire Spheres	
3.4 Sample Preparation	
3.5 Generating and Measuring Pressure	
4. ALIGNMENT AND MEASUREMENT	56
4.1 Alignment of Beam with the SBC	
4.2 Hitting the Sample with the Laser	

4.3	The Reflected Beam and the Signal at the Photodetector	
4.4	Determining the Correction Constant A	
4.5	Taking a Measurement	
4.6	Initial Measurements	
5.	CONCLUSIONS	67
5.1	Concluding Remarks	
5.2	Recommendations for Future Research	
	APPENDIX A	70
	BIBLIOGRAPHY	71

LIST OF FIGURES

Figure

1.1	Kerr Rotation versus Wavelength	1
1.2	Shift of the Kerr Peak	3
1.3	Electro-Magnetic Wave	4
1.4	Special Cases of Polarized Light	6
1.5	Polar, Transverse, and Longitudinal Kerr Effect	9
1.6	Electronic Level Splitting	10
1.7	Kerr Ellipticity Upon Reflection	11
1.8	Kerr Rotation Upon Reflection	12
1.9	Reading a Bit on a Magneto-Optical Disk	14
1.10	Writing a Bit into a Magneto-Optical Disk	15
2.1	Optical Table Setup for Measuring the Longitudinal Kerr Effect	18
2.2	Setup of Electronic Components	20
2.3	Polarity Switch Electronics	21
2.4	Reverse Galilean Beam Expander	24
2.5	Spherical Aberration and the Airy Pattern	26
2.6	Vibration of the Silica Bar	28
2.7	Retardation of Light through the PEM	29
2.8	Intensity of the Reflected Light	33
2.9	The First Three Bessel Functions	37
3.1	Diamond Anvil Cell	39
3.2	Basic Schematic of the SBC	40
3.3	Sapphire (Al_2O_3)	
	a) C-axis Vertically Oriented	43
	b) Plane Perpendicular to C-axis	44
3.4	Determining the C-axis	45
3.5	Bulls Eye Pattern	45
3.6	Chemical Mechanical Polisher	47
3.7	Epoxy Mount (~1 inch dia.)with Sapphire Sphere	49
3.8	Creating the Sample Flats	51
3.9	Sample Flat Under 5X Microscope	51
3.10	Optical Multichannel Analyzer (OMA)	55
4.1	A Direct Image (Left) and Projected Image (Right) of Sample	57
4.2	Simple Compound Microscope	58
4.3	Microscope Setup	60
4.4	Hysteresis Curve for BiYG Film	66

ABSTRACT

EXPERIMENTAL SETUP FOR MEASURING THE MAGNETO-OPTICAL KERR EFFECT UNDER HIGH ISOTROPIC PRESSURE

by

BRIAN CHRISTOPHER DONEHEW, B.S., M.S.

Southwest Texas State University

December 2001

SUPERVISING PROFESSOR: Wilhelmus Geerts

I investigated the optimal experimental setup for measuring the magneto-optical(MO) Kerr Effect under high isotropic pressure. Currently, most MO digital data storage devices use red laser light to read/write data. Theoretical calculations predict that MO materials will show a larger Kerr Effect at shorter wavelengths if placed under high pressure.¹ If shorter wavelength lasers could be used in data storage devices, data density might be increased 2-3 times. A brass sapphire ball cell(SBC), similar to a diamond anvil cell, is used to create the isotropic pressures. Theoretically, up to 2 GPa of pressure may be created. The Kerr Effect is measured using an intensity-stabilized laser, a photo-elastic modulator, and an electromagnet. This setup is normally used to measure the hysteresis curves for thin films, but the hysteresis curves can be rescaled to show Kerr Rotation or Kerr Ellipticity as a function of applied magnetic field. I investigated various issues including alignment, sample creation and preparation, chemical mechanical polishing of the sapphire spheres and creation of the gaskets, calibration of the setup, measuring pressure, and optimizing pressure in the chamber.

Chapter 1

Introduction and Theory

1.1 Focus of Research

This thesis focuses on research to increase the data density of magneto-optical data storage devices, thus increasing the efficacy of this technology.

One of the main limitations to data density in magneto-optical storage devices is the spot size of the laser. Magnetic domains that are smaller than the laser spot size cannot be read. More accurately, their signal is mixed in with the signals from adjacent domains, producing noise. Most magneto-optical materials show a more pronounced Kerr effect for red light than for shorter wavelengths. Consequently, red laser light is used to read data on a magneto-optical storage device. Below is a graph depicting the measured Kerr Rotation for iron over a range of photon energies from infrared light (<1.0 eV) up to ultraviolet light (5 eV). Note that the maximum absolute Kerr Rotation occurs for red light. In this thesis, the wavelength of light that shows the maximum Kerr Rotation is called the Kerr peak.

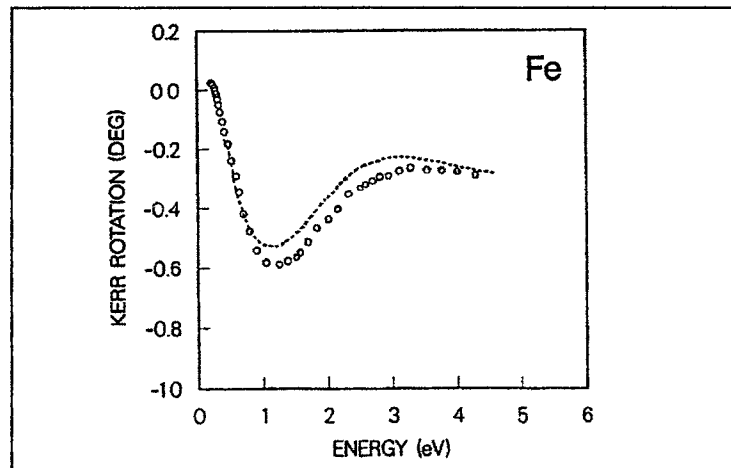


Figure 1.1 Kerr Rotation versus Wavelength¹

The minimum spot size for red light is greater than the minimum spot size for blue light, or for any other shorter wavelength. According to the Rayleigh criteria, spot size is proportional to wavelength. In other words, as the wavelength of the laser becomes smaller, the minimum spot size of the laser also decreases.

The Rayleigh criteria: $S = \lambda / N_A$

Where S = spot size

λ = wavelength of laser

N_A = numerical aperture of the lens system

If the Kerr peak for magneto-optical materials could somehow be shifted into the blue, then blue lasers could be used in magneto-optical hard drives. The blue laser, having a smaller spot size, could read smaller domains. Data density could be increased 2-3 times over its current value.

The Kerr Effect is dependent on spin-orbit coupling and the magnetization of the domains. However, the work of Dr. Oppenheimer, et al, suggests that lattice spacing may also influence the Kerr Effect. Dr. Oppenheimer and associates have made first principles calculations to evaluate the relationship between lattice spacing and the Kerr Effect. Their theoretical models for nickel show a significant shift in the Kerr peak (~ 1 eV) if the lattice spacing is increased by 5.9%.¹ This shift is towards the red wavelengths, and is shown in Figure 1.2. It is logical to suspect that if the lattice spacing is decreased, the Kerr peak will shift towards bluer wavelengths. One way to decrease the lattice spacing in a material is to place it under high pressure.

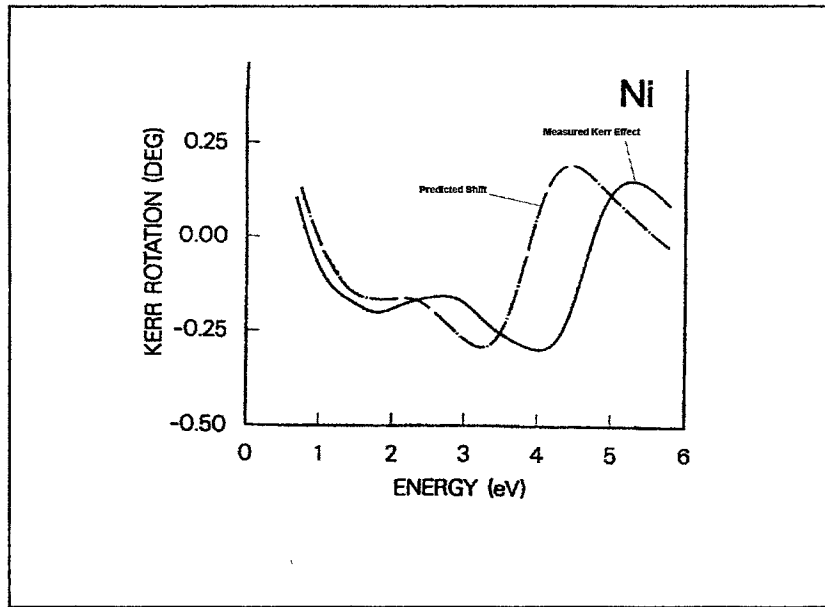


Figure 1.2 Shift of the Kerr Peak¹

The focus of the research in this thesis is to develop an experimental setup to measure the influence that high pressure has on the Kerr Effect for magneto-optical materials. The materials are placed under high pressure in a sapphire ball cell. The Kerr Effect for each material was measured with a laser using a technique originally developed to measure complex indices of refraction.

1.2 Polarization of E-M Waves

Light is a travelling electromagnetic (E-M) wave. An E-M wave is composed of an oscillating electric (E) and magnetic (B) field. The E-field and B-field are perpendicular to each other, and both are perpendicular to the direction of propagation (Figure 1.3). In general, the E-field interacts more strongly with materials than the B-field. For polarization, only the E-field component is considered.

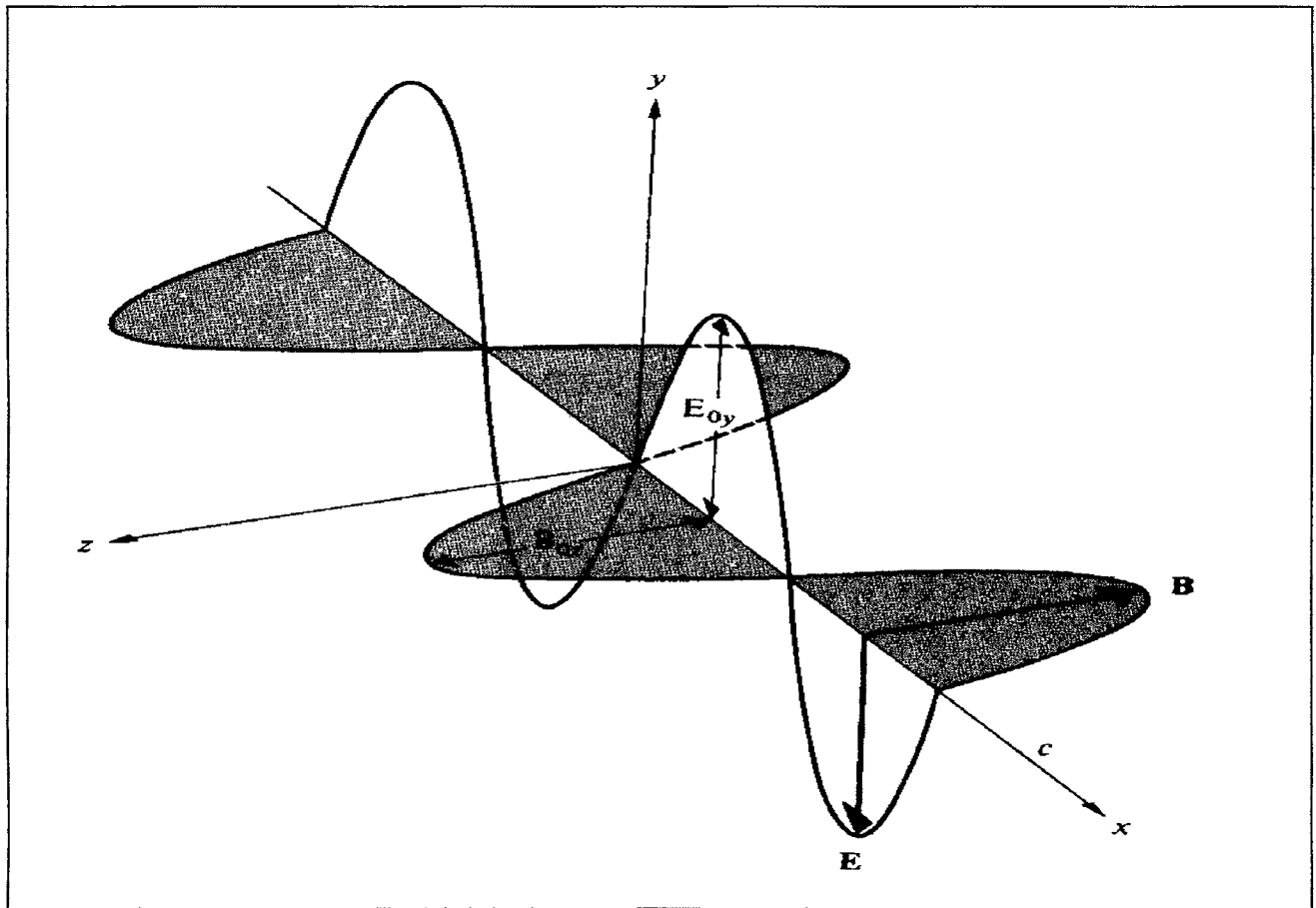


Figure 1.3 Electro-Magnetic Wave²

For most light sources, the E-fields of the individual photons are randomly oriented with respect to each other. This is *unpolarized light*. If, however, the E-fields of the light are made to be oriented in the same direction, the light is *polarized*. Polarized light can occur naturally (through reflection, for example), or unpolarized light can be made polarized through polarization filters.

The electric field of polarized light can be described with the following equation.

$$E(z, t) = \begin{bmatrix} E_x \cos(\omega t - 2\pi z / \lambda + \delta_x) \\ E_y \cos(\omega t - 2\pi z / \lambda + \delta_y) \end{bmatrix}$$

Where the wave propagates along the positive z-direction and

E_x = maximum component of the E-field in the x-direction

E_y = maximum component of the E-field in the y-direction

λ = wavelength of the light

ω = angular frequency of the light

δ_x = phase shift of E_x at $t = 0$

δ_y = phase shift of E_y at $t = 0$

For polarization, the behavior of the E-field is what is of interest. The actual position of the wave has little bearing on understanding the polarization, so let $z = \text{zero}$. In addition, due to the sinusoidal behavior of the wave, the time dependent part of the equation can be suppressed. This simplifies the above equation to

$$E = \text{Re} \begin{bmatrix} E_x e^{i\delta_x} \\ E_y e^{i\delta_y} \end{bmatrix}$$

This is the *Jones vector* for an E-M wave. Jones matrices are used to describe polarized light because they contain complete information about the amplitude and phase difference of the E_x and E_y component of the light wave's electric field. In general, only the difference between δ_x and δ_y is of interest, so one of them (usually δ_x) is often assumed to be zero.³

The figures below show the behavior of the E-field for some special cases. The vantage point is from the direction of propagation and looking into the E-M wave. The Jones vector for the wave is also given for each case.

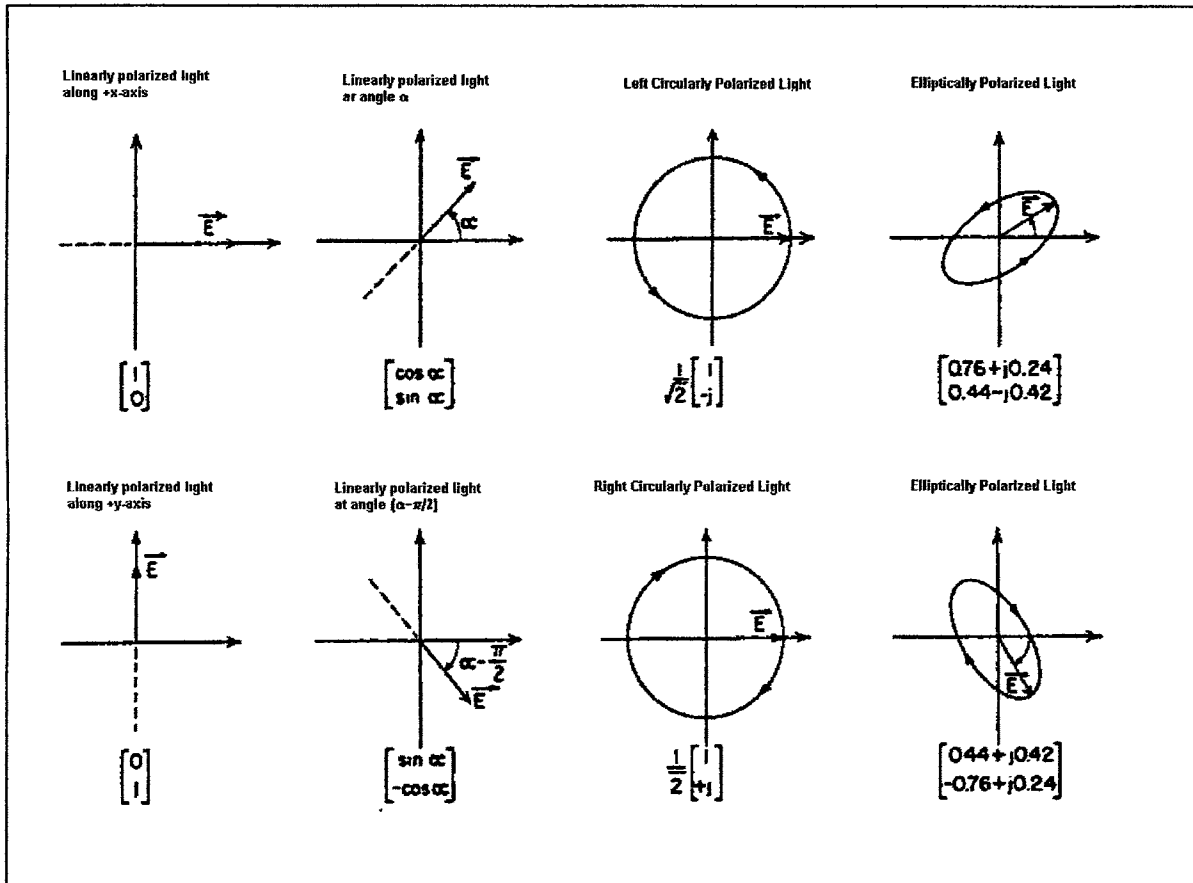


Figure 1.4 Special Cases of Polarized Light³

For linearly polarized light, there is no phase difference between E_x and E_y ($\delta_x - \delta_y = 0$). For right circularly polarized (RCP) light, E_x lags behind E_y by 90 degrees. For left circularly polarized (LCP) light, E_x leads E_y by 90 degrees. For both RCP and LCP light, E_x equals E_y . Qualitatively, for RCP light, the E-field rotates in a clockwise direction over time. The E-field for LCP light rotates in a counterclockwise direction over time. If E_x does not equal E_y , or if the phase difference between E_x and E_y is not

-90, 0, or 90 degrees, the light is elliptically polarized. The E-field traces out an ellipse over time.

1.3 The Kerr Effect – Macroscopic Description

When polarized light reflects off a magneto-optical material, both the ellipticity and the orientation of the polarization will change. This is the *Kerr Effect*. The change in the ellipticity of the light is the *Kerr Ellipticity*, and the change in the orientation of polarization is the *Kerr Rotation*. All polarized light can be thought of as the superposition of a right circularly polarized wave with a left circularly polarized wave. The Kerr Effect is due to a difference in the reflectivity of RCP light versus LCP light. The reflectivity is related to the Kerr Ellipticity and the Kerr Rotation by

$$\chi = F^+/F^- = \frac{(N^+ - 1)/(N^+ + 1)}{(N^- - 1)/(N^- + 1)} = \frac{1 + \tan \epsilon_K}{1 - \tan \epsilon_K} * \exp(-2i\theta_K)$$

- where
- χ = polarization variable
 - F^+ = amplitude of Fresnel reflection coefficient for RCP light
 - F^- = amplitude of Fresnel reflection coefficient for LCP light
 - N^+ = complex refractive index for RCP light
 - N^- = complex refractive index for LCP light
 - ϵ_K = Kerr Ellipticity angle
 - θ_K = Kerr Rotation angle

Therefore, as a result of the Kerr Rotation and Kerr Ellipticity, the reflected light will also change in intensity as the incident light changes its polarization.

The complex index of refraction, N , is related to the dielectric constant, ϵ , by

$$N^{+/-} = \sqrt{\epsilon^{+/-}}$$

In most materials the dielectric tensor is given, in Cartesian coordinates, by

$$\epsilon = \begin{pmatrix} \epsilon_{xx} & 0 & 0 \\ 0 & \epsilon_{yy} & 0 \\ 0 & 0 & \epsilon_{zz} \end{pmatrix}$$

However, in a magneto-optical material with a crystal structure of high symmetry (i.e. cubic), and with magnetization along the z-axis, the dielectric tensor is given by

$$\epsilon = \begin{pmatrix} \epsilon_{xx} & +\epsilon_{xy} & 0 \\ -\epsilon_{xy} & \epsilon_{xx} & 0 \\ 0 & 0 & \epsilon_{zz} \end{pmatrix}$$

The off diagonal non-zero terms are the origin of the Kerr Effect. Relating the index of refraction to the dielectric tensor leads to

$$(N^{+/-})^2 = \epsilon_{xx} \pm i\epsilon_{xy}$$

More importantly, in the case of small θ_k and ϵ_k , the relationship between Kerr Rotation, Kerr Ellipticity and the elements of the dielectric tensor are given by

$$\theta_k + i\varepsilon_k = \frac{\varepsilon_{xy}}{(1 - \varepsilon_{xx})\sqrt{\varepsilon_{xx}}}$$

For a more detailed description of the relationship between the dielectric tensor and the Kerr Effect, see the theses of H. Feil and W. Van Drent listed in the bibliography.

1.4 Orientation of the Magnetic Domains

The orientation of the magnetic domains in a material affects the RCP and LCP reflectivity of the material, and therefore affects the Kerr Effect (see Figure 1.5). If the domain orientation is in the plane of incidence and in the plane of the surface, a *longitudinal Kerr Effect* results. The maximum Kerr Rotation in this case is about four minutes of arc, and occurs at an angle of incidence of around 60 degrees. If orientation of the domains is perpendicular to the plane of incidence but in the plane of the material,

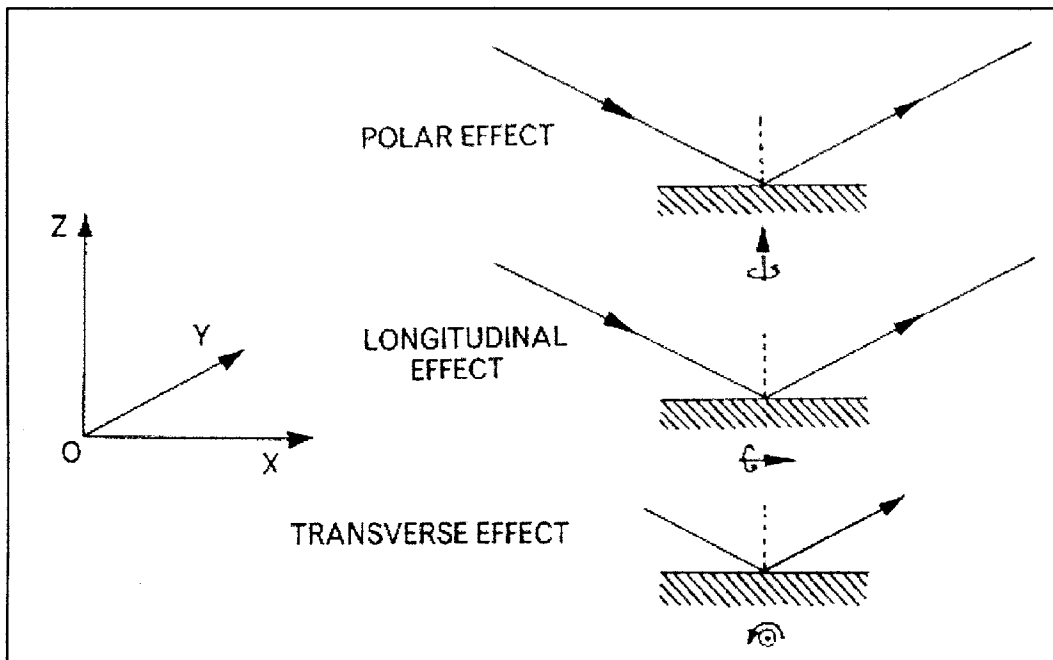


Figure 1.5 Polar, Transverse, and Longitudinal Kerr Effect⁴

a *transverse Kerr Effect* results. The Kerr Rotation in this case is similar to that of the longitudinal Kerr Effect. If the domain of orientation is perpendicular the surface of the material, the *polar Kerr effect* results. In this case the maximum Kerr Rotation may be up to 20 minutes of arc, and occurs when the angle of incidence equals zero degrees.⁴

1.5 Kerr Effect – Microscopic Description

Absorption, and therefore reflection, of light is caused by interband and intraband electron transitions in a material. In general, in individual atoms with more than one electron, electron energy is determined by the electron's principal quantum number n , and the angular momentum quantum number l . This leads to degeneracy in the electron energy levels, where electrons with different values of m_l and m_s have the same energy. If the atom is placed in a weak magnetic field, each energy level is split in two. The electrons having $m_s = +1/2$ go into one of the energy levels, and electrons having $m_s = -1/2$ go into the second energy level. In addition, for magnetic-optical materials, spin-orbit coupling causes these energy levels to further split according to the m_l quantum number, as in Figure 1.6. This phenomenon is known as the *Zeeman Effect*.

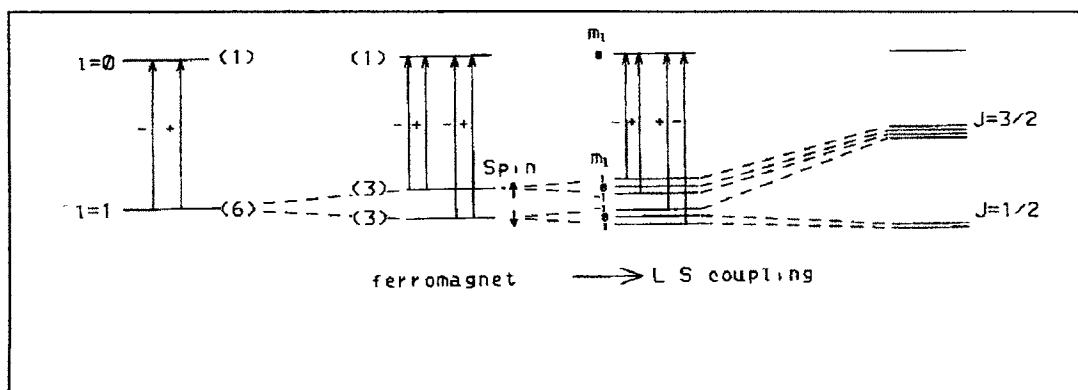


Figure 1.6 Electronic Level Splitting³

This split in the energy levels also occurs in the energy bands of magneto-optical materials. For magneto-optical materials, the selection rule for electronic transitions differs for RCP and LCP light. For RCP light, $\Delta m_l = +1$, and for LCP light, $\Delta m_l = -1$.³ Consequently, the reflectivity of RCP light is different from the reflectivity of LCP light. After reflection, the change in the magnitude of the E-field for RCP light differs from the change for LCP light. This change in the E-field's magnitude leads to a change in the ellipticity of the light. This is the origin of Kerr Ellipticity. Figure 1.7 shows a graphical representation of Kerr Ellipticity.

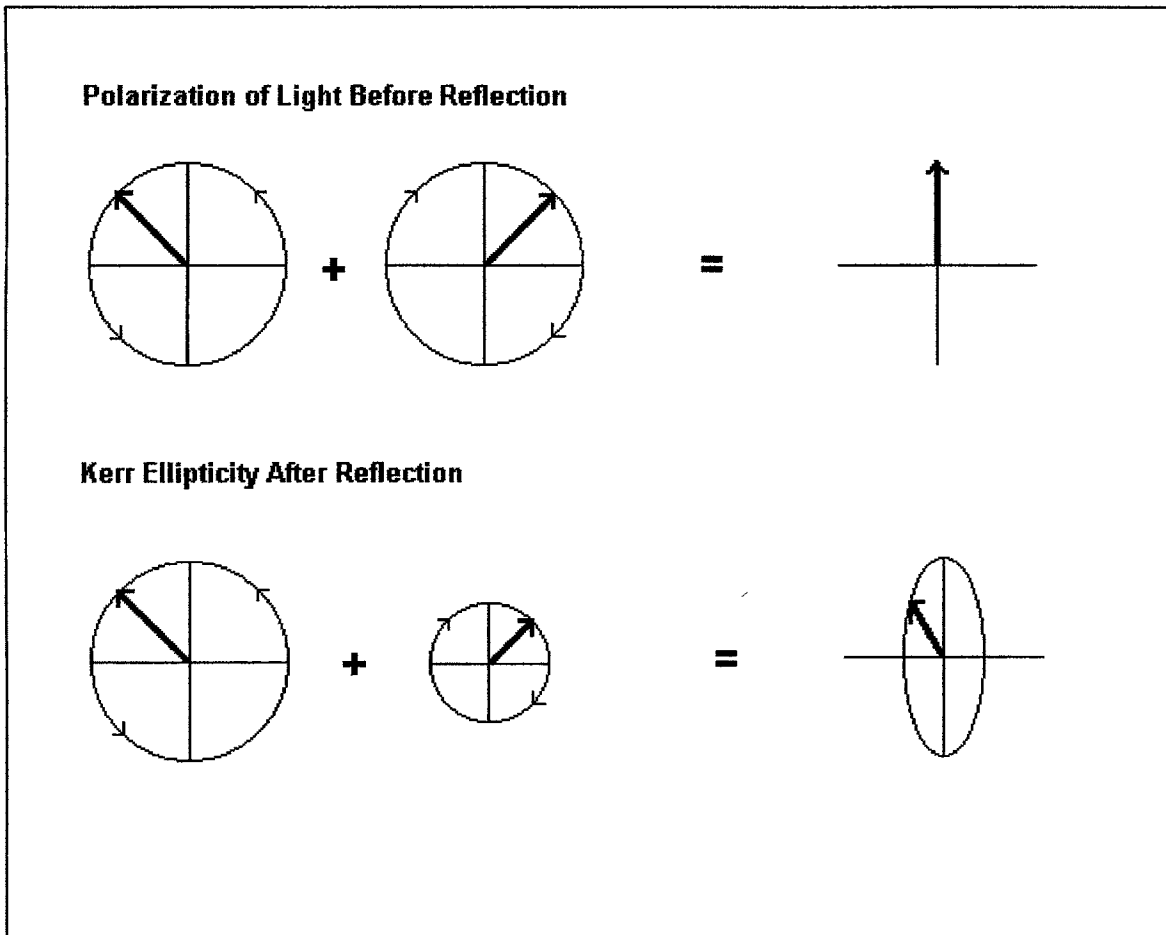


Figure 1.7 Kerr Ellipticity Upon Reflection

Kerr Rotation (see Figure 1.8) is also the result of the difference in absorption between RCP and LCP light. A phase shift occurs between the two components. The E-field of the combined RCP and LCP light will reach a maximum (i.e. their E-fields will “line up” with each other) along a different axis of polarization

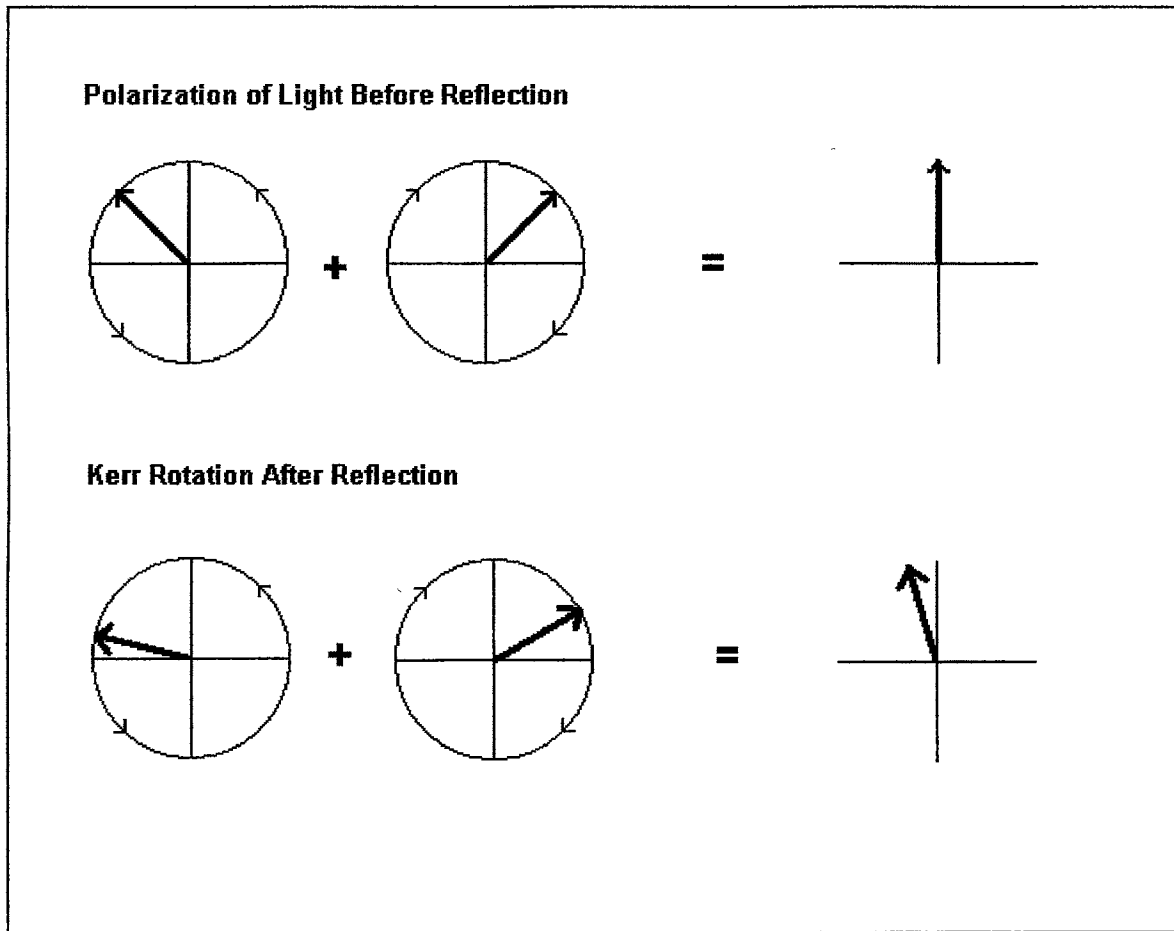


Figure 1.8 Kerr Rotation Upon Reflection

1.6 Applications of Magneto-Optical Materials

Digital data storage is one of the many applications for magneto-optical materials. In this application, a laser reads data stored on a magneto-optical disk. The data is in the form of magnetic domains on the disk. Depending on the orientation of its magnetization, a magnetic domain is either a ‘1’ bit or a ‘0’ bit.

Currently, most hard drives are standard magnetic hard drives. In order for magneto-optical storage devices to be a viable alternative to magnetic hard drive technologies, it must be competitive in both price and capability, while offering other advantages. A standard magnetic hard drive uses an electric coil to write data onto the hard drive and a magneto-resistor to read data on the hard drive. When a current flows through the electric coil, it produces a magnetic field that is strong enough to reverse the orientation of a magnetic domain. In this way data is changed or written. The resistance of a magneto-resistor changes as it moves through a magnetic field. As the magneto-resistor passes over a domain, its resistance will either decrease or increase depending on the orientation of the domain. In this way, a '1' bit can be differentiated from a '0' bit.

In contrast, a magneto-optical hard drive uses a laser to read data, and the combination of the laser plus an electric coil to write data. The domains in a magneto-optical hard drive are perpendicular to the plane of the hard drive. The laser strikes the hard drive at a right angle. The beam first travels through a transparent film, which focuses the beam down to less than a micrometer. The beam then reflects off a single domain. The polar Kerr Rotation for the laser depends on the orientation of the domains. The data is read by measuring the polar Kerr Rotation for the laser. For example, a clockwise Kerr Rotation may be a '1' bit, while a counter clockwise Kerr Rotation would be a '0' bit. Figure 1.8 shows a laser head reading a magnetic bit.

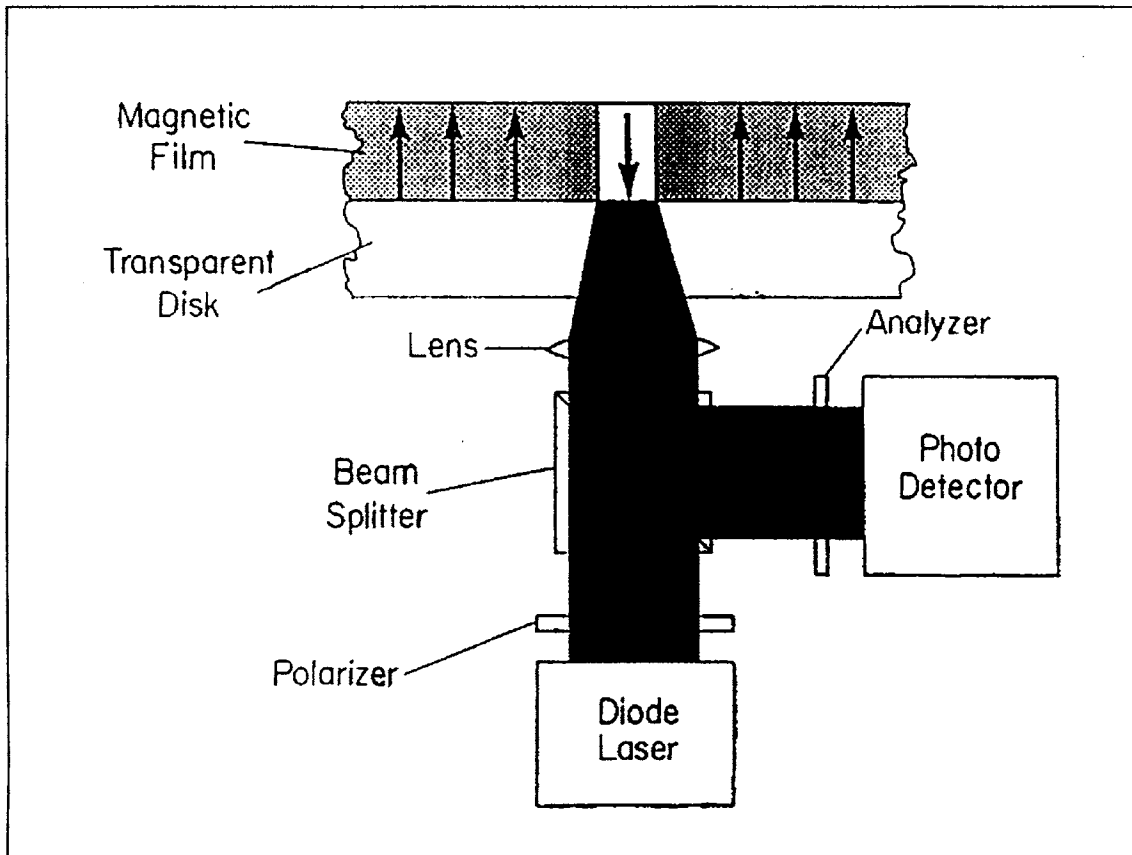


Figure 1.8 Reading a Bit on a Magneto-Optical Disk⁵

At room temperature, magneto-optical materials have high coercivities, and the magnetic field produced by an electric coil is not sufficient to flip the orientation of a domain. To write data on the disk, the laser first heats the domain to between 200-300 degrees Celsius. At this temperature, the coercivity of the material is much smaller. The electric coil can then be used to switch the orientation of the domain.⁵ Figure 1.9 shows the process of writing a bit.

Magneto-optical hard drives have two primary advantages over conventional magnetic hard drives. The first advantage for magneto-optical storage devices is their durability. At room temperature, they have very high coercivities. The orientation of the

magnetic domains is relatively impervious to stray electromagnetic fields, thermal excitation, or rough handling of the data disk. This makes magneto-optical storage

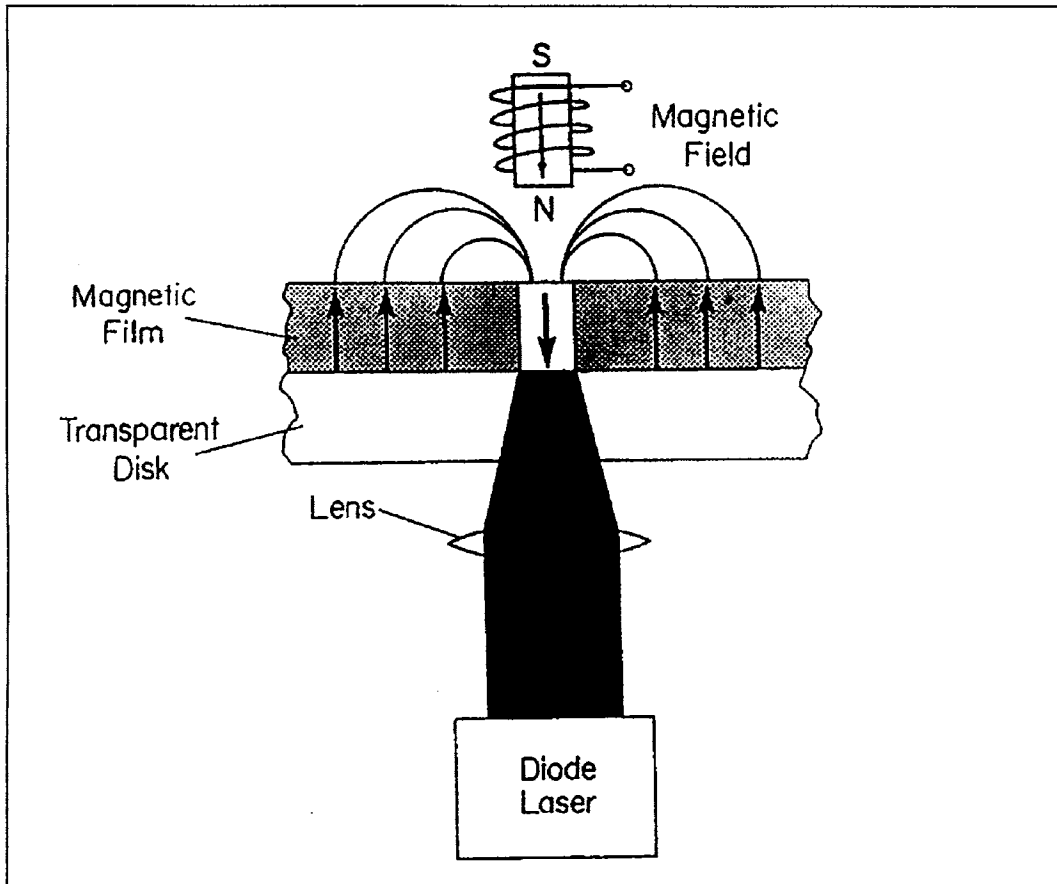


Figure 1.9 Writing a Bit Into a Magneto-Optical Disk⁵

devices ideal for archiving data. Secondly, conventional magnetic hard drives require the read and write head to travel at high speeds only a few hundred nanometers above the surface of the hard drive. If there is any particle contamination on the hard drive or if the hard drive is roughly handled, the head can crash into the disk. This risk is greatly reduced in magneto-optical hard drives, where the distance from the disk to the laser is much greater. Magneto-optical disks combine the durability and portability of floppy

disks and zip-disks with a data storage capacity within an order of magnitude of many magnetic hard drives. They are also faster and more energy efficient than read/recordable compact disks.

Chapter 2

Experimental Setup

2.1 Setup of the Optical Table for Measuring the Longitudinal Kerr Effect

The optical table equipment should be laid out as in Figure 2.1, which is a top-down view of the optical table. A Melles Griote Model 05 STP901 produces a 632.8 nm laser beam. Using an adapter, a Zoom Beam Expander from Edmund Scientific is attached to the front of the laser. The beam expander increases the diameter of the laser beam and decreases its divergence. After passing through the beam expander, the width of the laser beam is approximately one cm. For a more detailed description of the laser and beam expander, see chapter 2, Section 4. The beam then passes through a quarter wave plate. The quarter-wave plate causes a 90-degree phase shift between the E-component parallel to its transmission axis and the E-component perpendicular to this axis. Since the laser light is polarized, by rotating the quarter-wave plate, the intensity of the beam can be adjusted. The polarizer is set at 45 degrees from horizontal. The polarizer transmits the component of the laser beam that is parallel to the transmittance axis. Therefore, the beam that enters the photoelastic modulator (PEM) is linearly polarized at 45 degrees from horizontal. In other words, after the beam passes through the polarizer, it has equal s- and p-components. Both the polarizer and analyzer are Glan-Taylor U-V prism polarizers, model MGTYS15, from the Karl Lambrecht Company. The PEM (model PEM-90 from Hinds Instruments) contains a crystal that expands and contracts at a rate of 50 KHz. As the light travels through the crystal, the oscillating crystal structure causes a phase shift between the s- and p-components. The net effect is that, after leaving the PEM, the laser beam shifts from RCP light to LCP light and back

again at a rate of 50 KHz. See chapter 2, Section 5, for a more detailed description of the PEM.

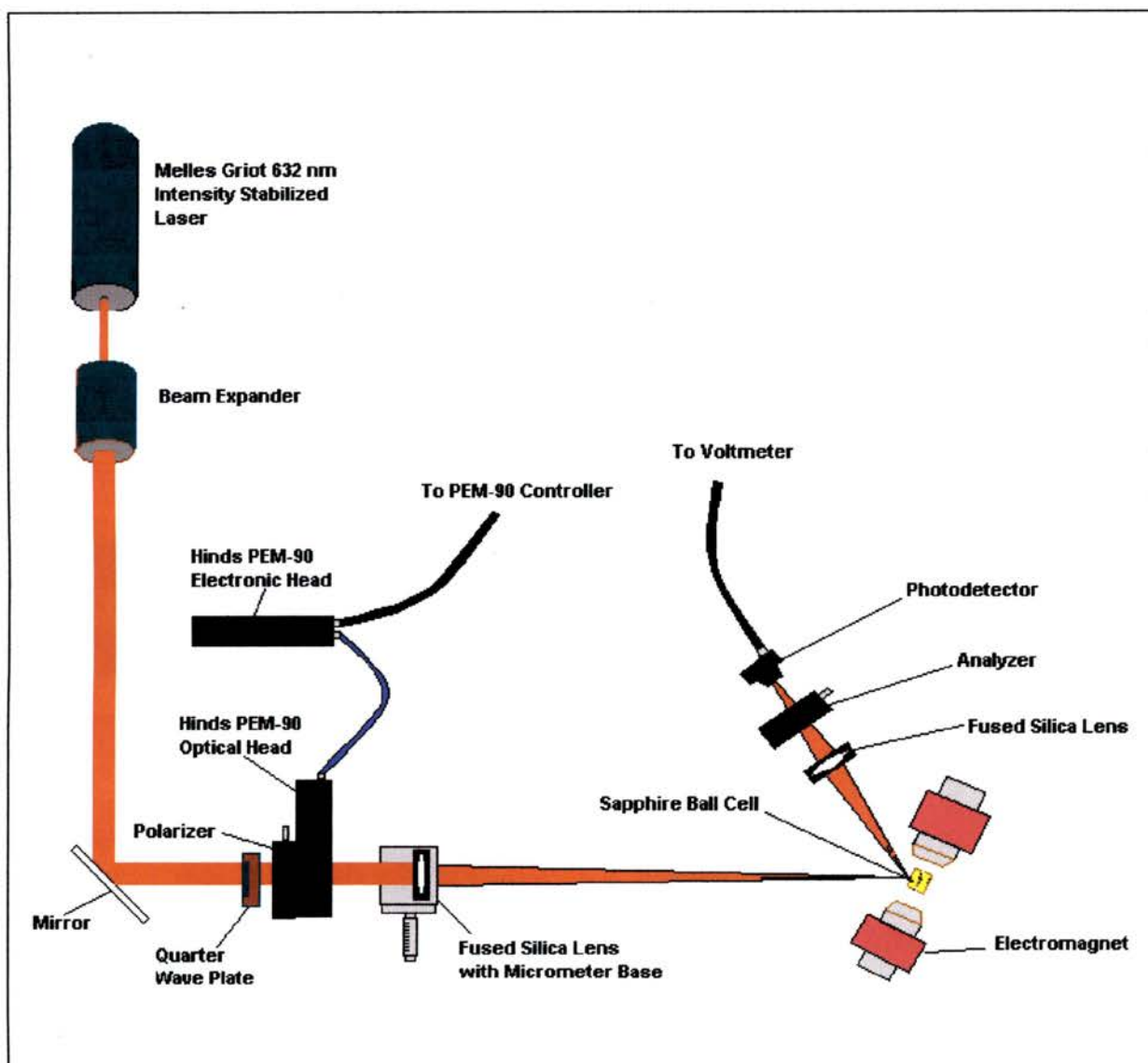


Figure 2.1 Optical Table Setup for Measuring the Longitudinal Kerr Effect

The laser beam then passes through a fused silica lens with a focal length of 200 mm. Because it is made of fused silica, the lens does not produce an unwanted change in the state of polarization of the laser light. The lens, in combination with the beam expander, reduces the laser beam to its smallest possible spot size at the lens' focal

length, while preserving intensity. A 3-D micrometer base has been constructed that allows fine adjustment of the lens position. The lens can then be used to aim the laser beam onto the sample in the Sapphire Ball Cell (SBC). The SBC and the Cenco Instruments 60V electromagnet are placed at the focal length. The magnet is capable of producing fields up to 700 gauss. The SBC and the magnet should be tilted at a maximum angle of ten degrees from perpendicular to the beam. The SBC should be approximately halfway between the pole pieces of the magnet. Use either the Ardel Kinematic base or the 3-D micrometer base to hold the SBC between the pole pieces. Both allow for fine adjustment of the SBC's position. A model 912 gaussmeter manufactured by Magnetic Instruments, Inc. is used to measure the magnetic field between the pole pieces. A metal arm has been attached to the magnet to hold the gauss probe in position. After the beam reflects off the sample and exits the SBC, it should be at an angle of approximately 20 degrees from the incident beam. The reflected beam may diverge significantly, such that it is too wide to go through the analyzer. A fused silica lens can be used to contract the size of the reflected beam so it can pass through the analyzer. The transmittance axis of the analyzer should be along the horizontal, parallel to the surface of the optical table. Finally, the laser beam should strike the face of the Thorlabs, Inc. model PDA50 photodetector. For more information on the polarizer, analyzer, gaussmeter and photodetector, consult Patrick Holland's thesis "Magnetic Hysteresis Curves of Thin Films under Isotropic Stress."

2.2 Electronic Setup for Measuring and Analyzing Data

Figure 2.2 shows the connections for the electronic components, and Table 2.1 gives a list of the principle electronic components. The Lock-In Amplifier (LIA), Voltmeter, Gaussmeter, Magnet Power Supply, and Switching Unit are plugged into the

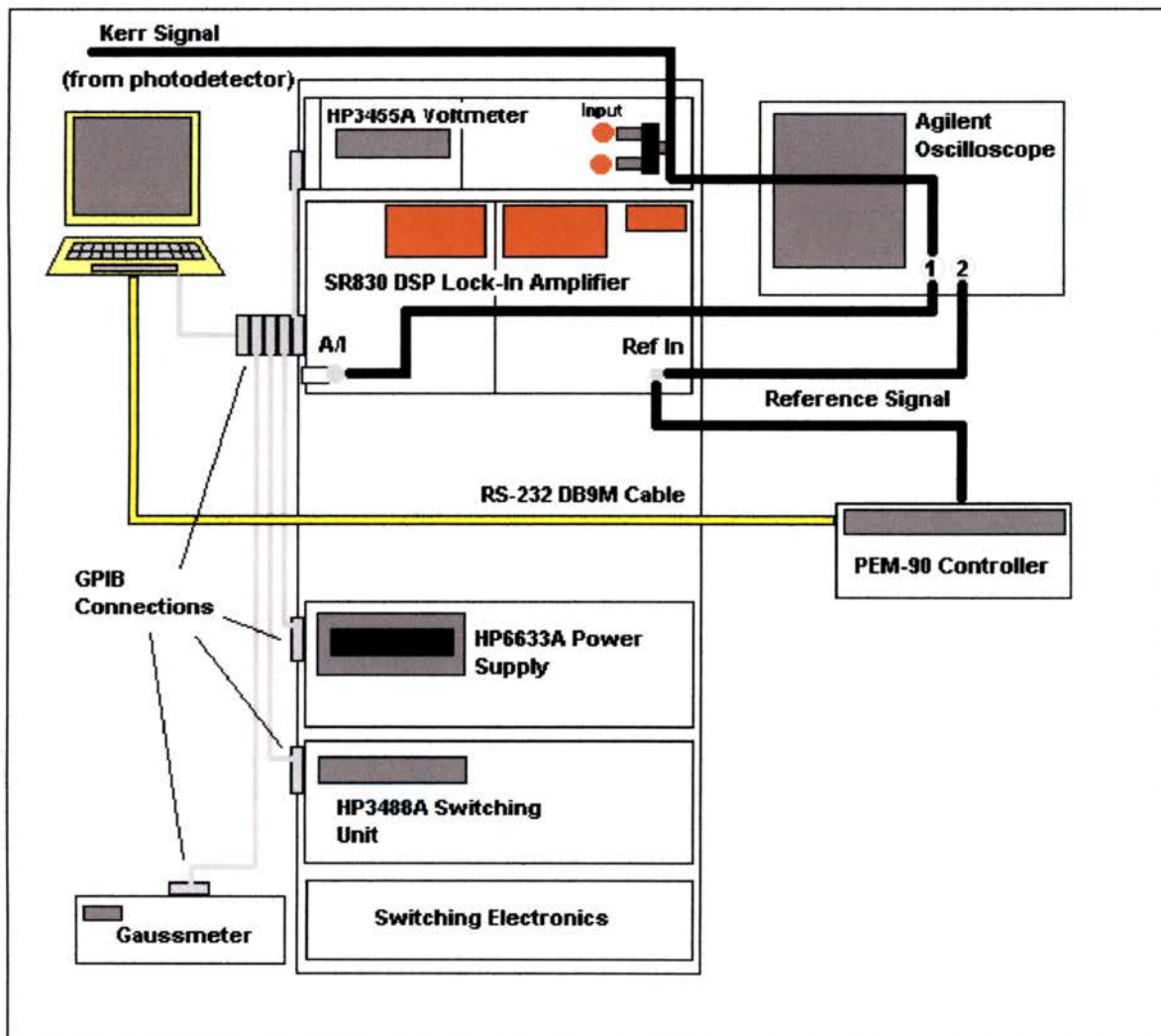


Figure 2.2 Setup of Electronic Components

GPIB port on the computer. The PEM controller is plugged into the left nine-pin port (RS-232 DB9M cable) on the computer. The LIA measures the AC components of the

photodetector signal. The voltmeter measures the DC component, which represents the intensity of the light beam. The DC power supply provides voltage and current for the electromagnet. The gaussmeter measures the magnetic field between the poles. All of these components interface directly with the computer. The switching unit, polarity switch and polarity switch power supply act as a unit to switch the polarity of the electromagnet (see figure 2.3). The switching unit interfaces with the computer, but its electronics are too delicate to handle the high current (1-2 amps) through the electromagnet. The polarity switch has relays that can handle the magnet current. When the voltage in the magnet is (nearly) zero, the switching unit instructs the polarity switch

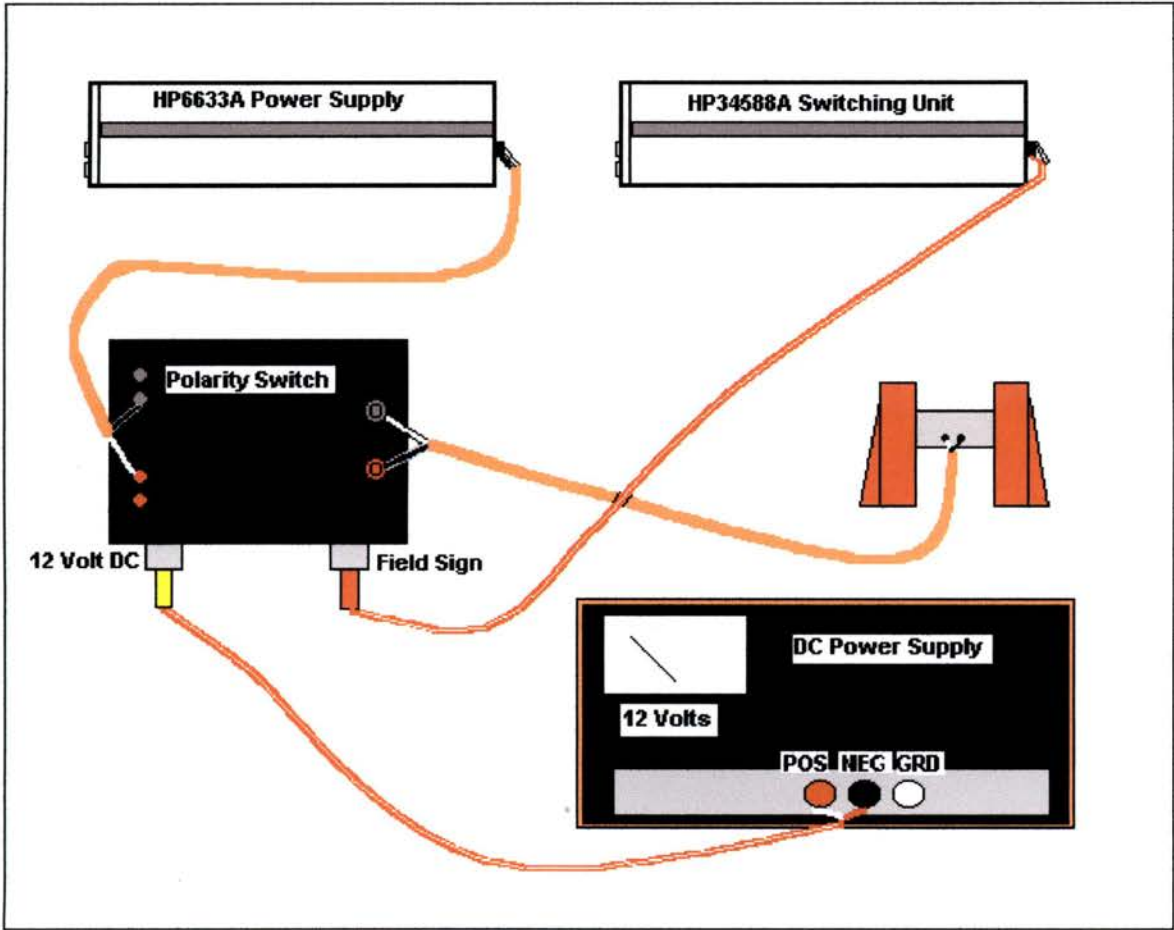


Figure 2.3 Polarity Switch Electronics

to flip its relays. This will switch the direction of current and flip the magnetic field created by the electromagnet. The setup for the switching electronics is shown below. The Polarity Switch Power Supply should be set to **12 Volts**.

Table 2.1 List of Electronic Components

Instrument	Model	Manufacturer
Lock-In Amplifier	SR830 DSP	Stanford Research Systems
DC Power Supply	HP6633A	Hewlett Packard
Digital Volt Meter	HP3455A	Hewlett Packard
Switching Unit	HP3488A	Hewlett Packard
Polarity Switch	One of a Kind	Southwest Texas State
Polarity Switch Power Supply	PLS50-1	Systron-Donner Corp.
Oscilloscope	54622D	Agilent
Computer	486	Dell

During a measurement, the computer software will control and/or monitor the LIA, voltmeter, gaussmeter, switching unit and magnet power supply. Use coaxial cables to carry the Kerr signal and reference signal from component to component. The Kerr signal from the photodetector must first go to the two input terminals on the voltmeter. A coaxial-double banana adapter will be necessary. The Kerr signal then goes to terminal "1" on the oscilloscope. From there, the signal should go to terminal "A/I" on the LIA. A 50 Ω resistor cap should also be placed on this terminal. The reference signal goes

from the “1f” terminal on the PEM to the “REF IN” terminal on the LIA. The reference signal should then go to terminal "2" on the oscilloscope.

2.3 Laser

The laser on the optical table is a model 05 STP901 manufactured by Melles Griot. A stabilized HeNe laser produces a highly stable beam of collimated, polarized, single mode, 632.8 nm wavelength laser light at stable frequency or stable intensity. Since the Kerr effect is calculated from small fluctuations in the intensity of the beam, the laser is operated in the intensity-stabilized mode. Once the laser is turned on, it takes approximately 20 minutes for the intensity to stabilize. The laser controller will make several clicking sounds to indicate that the intensity has stabilized.

For resonance of light to occur in the laser cavity, one round trip in the cavity must equal an integral number of wavelengths.

$$N \lambda = 2 L$$

Where N is an integer equal to the number of wavelengths, λ is the wavelength of light, and L is the cavity length. Each allowable wavelength is called a steady state longitudinal mode, and each mode is separated, in Hz, from its nearest neighbor by the value $c/2L$, where c is the speed of light. For this laser, the modes are separated by approximately 640 MHz.

The light emitted by the atoms in the plasma undergoes a Doppler shift due to the motions of the atoms. This leads to a Gaussian distribution in the emitted wavelengths.

The half-power width of this distribution is approximately 1400 MHz. There will be only two steady state modes within the half-power width; each separated by 640 MHz. In the intensity-stabilized mode, control circuitry monitors the intensity of one of the allowed modes and thermally controls the length of the cavity to maintain the intensity.⁶

2.4 Beam Expander and Focusing Lens

The Edmund Scientific Zoom Beam Expander is a reverse Galilean telescope (see Figure 2.4). The beam expander, as the name implies, increases the size of the beam diameter. However, it also decreases the divergence of the beam. The decrease in divergence is directly proportional to the increase in diameter. The Zoom Beam expander has a variable expansion power of 10X-20X. Because of the beam expander, the beam is more highly collimated when it reaches the fused silica lens, resulting in a

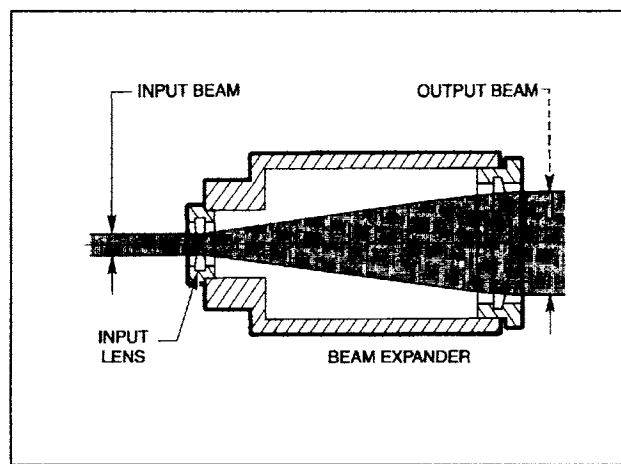


Figure 2.4 Reverse Galilean Beam Expander

cleaner spot at the sample. The beam expander can also be used to focus the beam at long distance. The Zoom Beam Expander has a variable focal point of 1.2 m to infinity.

The beam expander and the focusing lens work together to minimize the spot size of the beam at the sample. It is important that the laser beam only hits the sample during a measurement, and not “overlap” into the gasket or the SBC or anything else. The Kerr signal from the sample should not be mixed in with signals from the other materials in the SBC. The unmodified laser beam is approximately one mm in diameter, which is at least twice as large as the sample. The laser beam needs to be shrunk down to a size smaller than the sample. The photodetector measures changes in the intensity of the reflected beam. Therefore, the entire beam should continually strike the sample throughout the measurement. If the sample’s position with respect to the beam shifts during a measurement, a smaller spot size helps to ensure that the entire beam stays on the sample. The spot size produced by the fused silica lens is primarily determined by the spherical aberration of the lens and the f-stop number ($F/\#$) of the lens. Spherical aberration is the result of the spherical shape of the lens. Light that enters the lens near the central axis has a different focal point than light that enters the lens away from the central axis (Figure 2.5a). This causes an interference pattern known as an Airy pattern (Figure 2.5b). It is apparent from Figure 2.5 that, as the diameter of the laser beam decreases, the Airy pattern produced by spherical aberration also decreases. More of the laser light is concentrated around the central axis.

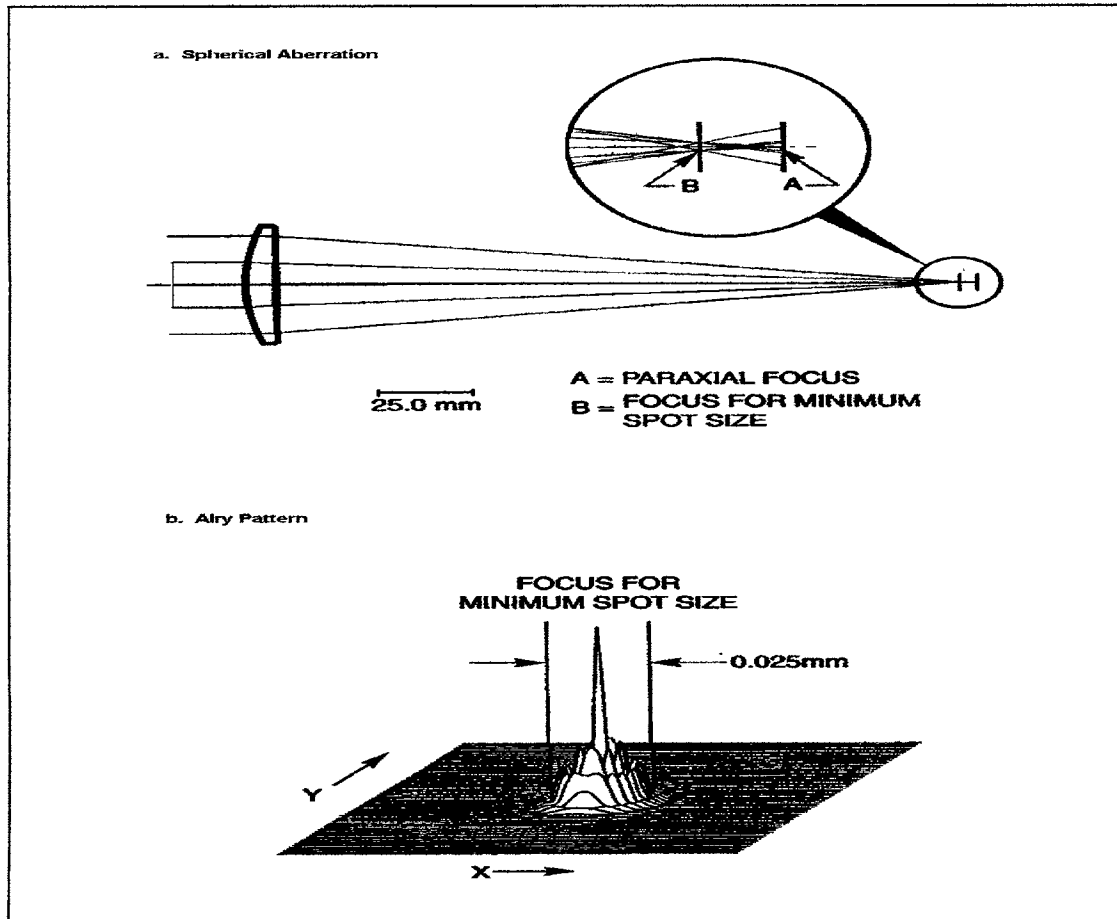


Figure 2.5 Spherical Aberration and the Airy Pattern⁷

The spot size of the laser at the sample is linearly dependent on the wavelength of the laser and the $F/\#$ of the focusing lens, where $F/\#$ is defined as

$$F/\# = \frac{\text{(focal length of lens)}}{\text{(diameter of laser beam)}}$$

The spot size at the sample is inversely related to the diameter of the laser beam. The beam expander controls the diameter of the beam, and can be used to change the $F/\#$ of the lens.¹⁶

When attempting to minimize the spot size, the spherical aberration and the F/# work in opposition to each other. A large diameter laser beam has a small F/#, and produces a small spot size, but produces a large Airy pattern. Conversely, a small diameter beam has a small Airy pattern, but due to its large F/#, it produces a large spot size. For a 200 mm lens (the kind used in the Kerr setup), Oriel, Inc. has calculated the F/# which optimizes these two factors to get the minimum spot size. Theoretically, a F/11 lens generates a spot size of 0.015 mm. This corresponds to a beam diameter of 18.2 mm.⁷

2.5 Photoelastic Modulator

A model PEM-90 photoelastic modulator manufactured by Hinds Instruments was used to modulate, at a fixed frequency, the polarization of the laser beam. The PEM consists of three components – the optical head, the electronic head and the controller, plus connecting cables. The electronic head and the optical head are connected by the triaxial cable. The electronic head is connected to the controller. **Never** operate the PEM unless the optical head is connected to the electronic head by the triaxial cable.

FAILURE TO DO SO CAN DAMAGE THE ELECTRONIC HEAD!

The light of the laser beam can be represented mathematically as the superposition of a horizontal x-component (E_x) and a vertical y-component (E_y). The state of polarization is determined by the relative phase of the two components. When the beam passes through a material, it may experience birefringence. The index of refraction of the E_x component and the E_y component may differ from each other. The velocities of the two components through the material will be slightly different, causing a

phase shift between them. The phase shift manifests as a change in the state of polarization.

To modulate the polarization of the light, the PEM uses the photoelastic effect, in which a mechanically stressed sample exhibits birefringence proportional to the resulting strain. The PEM-90 has a rectangular bar of fused silica attached to a piezoelectric transducer. The transducer causes the bar to vibrate along its long axis at its natural resonant frequency of about 50 KHz (see Figure 2.6).

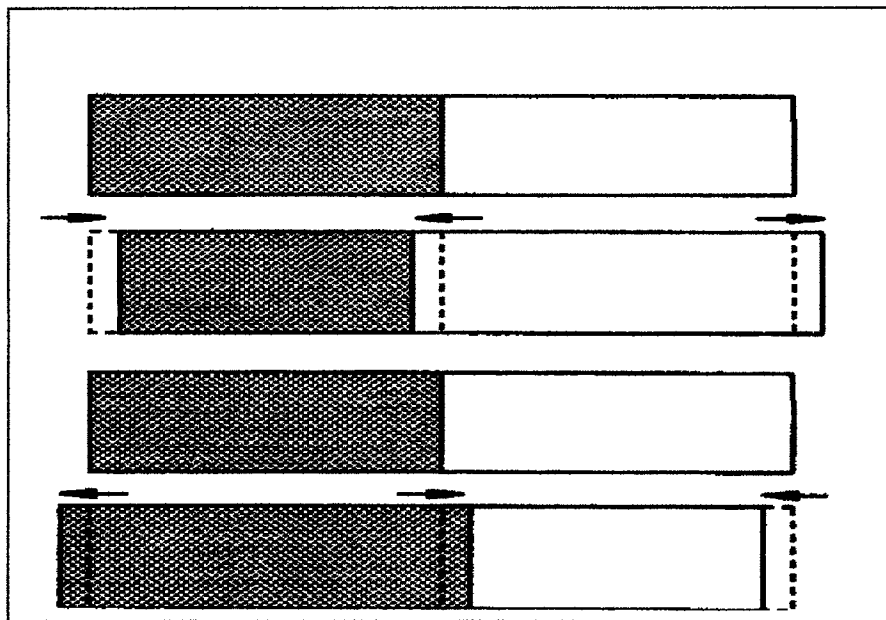


Figure 2.6 Vibration of the Silica Bar⁸

As the beam passes through the polarizer, it becomes linearly polarized at 45 degrees from horizontal. As the beam enters the PEM, the light has two components, E_x and E_y , both equal in magnitude and in phase with each other. The vibration of the fused silica bar is along the horizontal; parallel to the E_x component and perpendicular to the E_y component.

When the silica bar is relaxed (not stressed), the two light components are affected equally, and there is no change in polarization. When the silica bar is

compressed, the E_x component travels slightly faster through the bar than the E_y component. The E_x component then “leads” the E_y component upon exiting the PEM (see Figure 2.7). If the silica bar is stretched, E_x travels slightly slower through the bar than E_y . The E_x component “lags” behind the E_y component. The phase difference between the two components is called the retardation angle δ . The retardation angle as a function of time is given by

$$\delta(t) = \delta_0 \sin(2\pi p t)$$

where δ_0 is the maximum or peak retardation angle and p is the frequency of the PEM.⁸

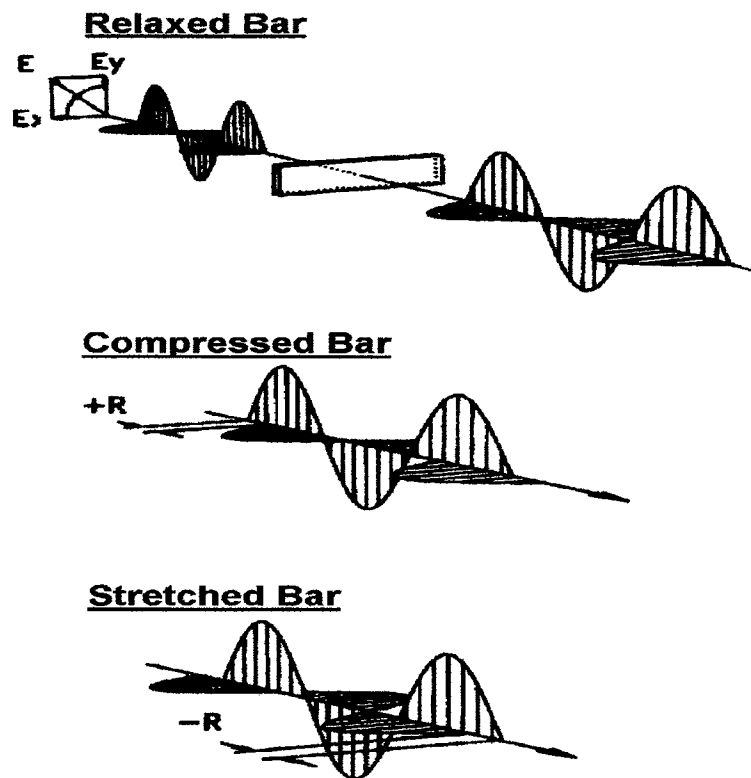


Figure 2.7 Retardation of Light through the PEM⁸

2.6 Lock-In Amplifier

A Lock-in Amplifier is used to measure small AC signals (down to a few nanovolts) that are buried within a noise signal which may be much larger. The LIA compares the incoming signal to a reference signal that has the same frequency as the desired signal. Ideally, the reference signal is created by the mechanism that creates the AC signal of interest. In the Kerr measurement setup, the piezoelectric transducer in the PEM generates the reference signal (a square wave at 50 KHz) and the oscillation in the laser beam's polarization (also at 50 KHz). The oscillation in the intensity of the beam is very small compared to the magnitude of the beam intensity, making it necessary to use the LIA to measure it.

According to Fourier's Theorem, any input signal can be represented by the sum of many AC signals (sine waves) of differing amplitudes, frequencies and phase angles. The LIA multiplies the reference signal by the input signal and integrates the product over time. Sine waves are orthogonal functions to each other unless they have same frequency. If two functions are orthogonal, then the integration of their product is zero, unless f_1 equals f_2 .⁹

$$\int \sin(f_1 t) \sin(f_2 t) dt = 0$$

By performing this integration, the LIA eliminates from the input signal all elements that do not oscillate at the reference frequency. Generally, only the AC signal of interest will have the same frequency. The integration of the two signals yields a DC signal. If

the magnitude of the reference signal is normalized, then the magnitude of the DC signal is the amplitude of the AC signal of interest.

2.7 Theory of Operation

2.7.1 Overview

The original purpose of this experimental setup was to take spectroscopic measurements of complex indices of refraction.¹⁰ This technique can also generate hysteresis curves for thin films and other samples with small magnetizations. This technique can measure magnetizations down to 10^{-9} or 10^{-10} emu.¹¹ By comparison, a Vibrating Sample Magnetometer (VSM) has a sensitivity of approximately 10^{-3} to 10^{-4} emu. Theoretically, the magnetization of a single layer of iron atoms could be measured. The magnetic moment of a single iron atom is approximately $4\mu_B$, where μ_B is the Bohr magneton (9.27×10^{-21} emu)³³. With a lattice spacing of 2.87 Angstroms, the magnetic moment of a single layer of iron atoms is about 1.13×10^{-5} emu/cm². For an expected laser spot diameter of about 0.05 mm, this translates to a magnetic moment of approximately 8.84×10^{-10} emu. This magnetic moment is just in the range detectable by this setup. The hysteresis curves generated by this method can be rescaled to show Kerr rotation or ellipticity as a function of applied magnetic field.

The sample is placed between the poles of the electromagnet. During a measurement, the magnetic field between the poles goes through one cycle from a maximum in one direction to a maximum in the other direction and back again. The magnetization in the sample changes with the imposed magnetic field. As the laser beam reflects off the sample, it undergoes the Kerr effect. The Kerr effect will change as the

magnetization changes. As described in chapter 2, Section 5, the PEM transforms the linearly polarized laser light into light that sinusoidally oscillates from RCP light to LCP light at a rate of 50 KHz. At a given applied magnetic field, the computer measures the fluctuating intensity of the reflected beam due to the change from RCP light to LCP light and back again.

2.7.2 Graphical Description of the Reflected Beam at the Photodetector

The analyzer only allows the horizontal component of the reflected light to reach the photodetector. The intensity of the horizontal component of the light will change sinusoidally with time if there is a Kerr Effect. After the laser beam emerges from the PEM, it is oscillating between RCP light and LCP light. The light incident on the PEM has its polarization axis at 45 degrees from the horizontal. In other words, the incident light has equal components in the horizontal and vertical direction ($E_x = E_y$). If the angle of retardation of the PEM equals 90 degrees, then the transmitted light will oscillate between RCP and LCP light with a period of $1/f$ seconds, where f is the frequency of the PEM¹²

Figure 2.8a shows the light of the reflected beam when there is no Kerr Effect. The vantage point is from the direction of propagation, looking into the beam. The top half shows the E-field of the light over one period of the oscillation. It is apparent that the state of polarization of the reflected beam is the same as that of the incident beam. The bottom half of Figure 2.8a shows the intensity of the horizontal component of the light over the course of one period of oscillation. With no Kerr Effect, the intensity of the horizontal component does change. Figure 2.8b shows a reflected beam that has

undergone Kerr rotation. In this situation, the Kerr Effect will not influence the state of polarization of RCP or LCP light, but will change the state of polarization of linear polarized light. The main axis of polarization is no longer at 45 degrees. Consequently, the horizontal component is no longer constant with time. As shown in Figure 2.8b, the intensity oscillates with a period of $1/(2f)$. Figure 2.8c shows a reflected beam that has undergone Kerr ellipticity. The RCP light has a different intensity than the LCP light (see also Chapter 1). Therefore, the horizontal component changes intensity in direct relation with the oscillation. The intensity oscillates with a period of $1/f$.

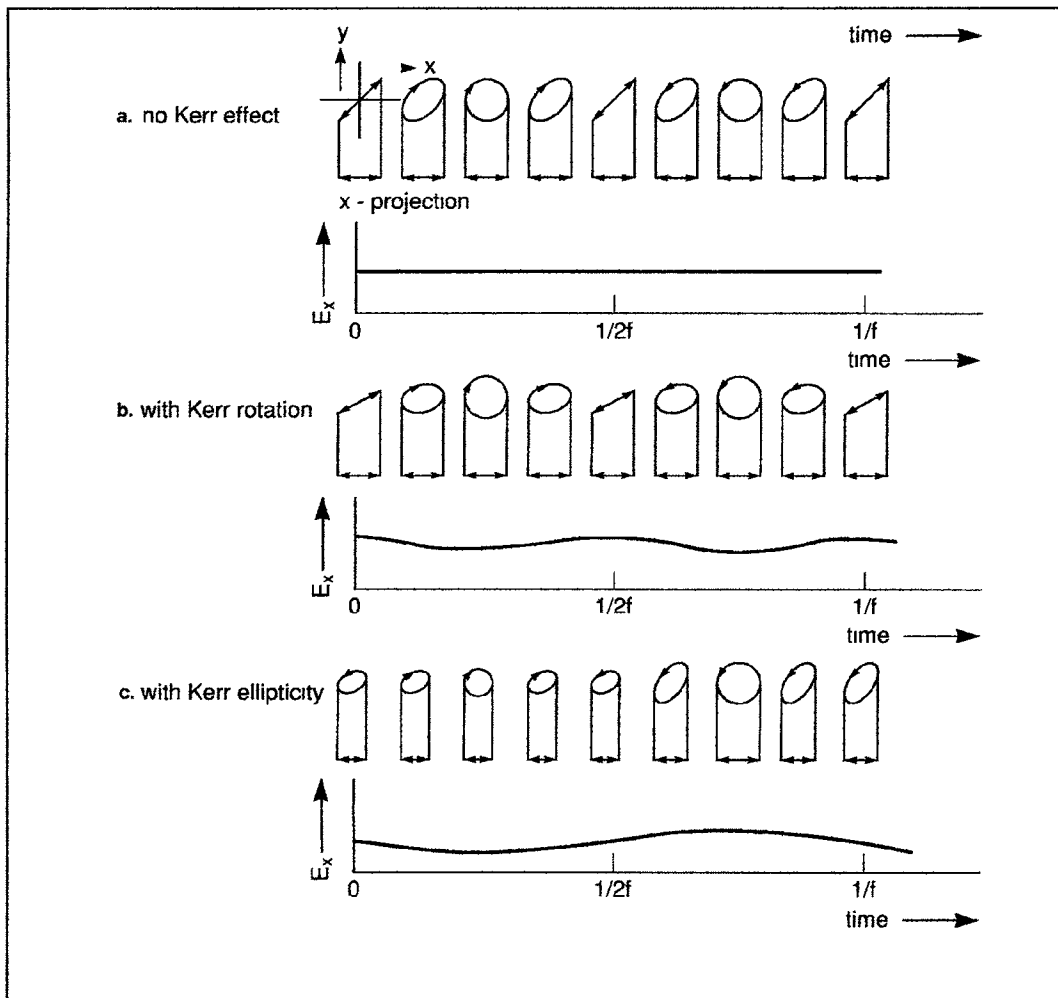


Figure 2.8 Intensity of the Reflected Light¹²

2.7.3 Analytical Description of the Intensity of the Reflected Beam

Assume the PEM has a retardation angle of δ_0 (in radians). As it leaves the PEM, the phase difference between the horizontal and vertical components of the laser beam will fluctuate according to

$$\delta = \delta_0 \sin(2\pi pt)$$

where p is the frequency of the PEM. The intensity of the light at the detector is

$$I = \frac{eE^2}{16\pi} \left\{ R + \frac{\Delta R}{2} \sin(\delta) + R \sin(\Delta\theta + 2\phi) \cos(\delta) \right\}$$

where

$$R = \frac{1}{2}(r_+^2 + r_-^2)$$

$$\Delta R = r_+^2 - r_-^2$$

$$\Delta\theta = \theta_+ - \theta_-$$

$r_{+/-}$ and $\theta_{+/-}$ are related to the Fresnel reflection coefficients of RCP (+) and LCP(-) light by

$$F^\pm = r_\pm e^{i\theta_\pm}$$

The assumption is made that $\Delta R/R \ll 1$.

Kerr rotation (θ_K) and Kerr ellipticity (ε_K) can then be expressed as

$$\theta_K = -\frac{\Delta\theta}{2} \qquad \varepsilon_K = \frac{\Delta R}{4R}$$

The intensity of the reflected beam at the photodetector is given by

$$I = I(O) + I(p)\sin(2\pi pt) + I(2p)\sin(4\pi pt) + \dots$$

$$I(O) = I_o R \{1 + J_o(\delta_o) \sin(\Delta\theta + 2\phi)\}$$

$$I(p) = I_o \Delta R J_1(\delta_o)$$

$$I(2p) = 2I_o R J_2(\delta_o) \sin(\Delta\theta + 2\phi)$$

$\Delta\theta$ is the phase change between the RCP light and the LCP light upon reflection, and ϕ is the angle of the analyzer. $I_o = (\varepsilon/8\pi)E^2$, and J_0 , J_1 and J_2 are the Bessel functions of the zeroeth, first and second order, respectively. For a more detailed description of this derivation of the relationship between the PEM, the intensity of the signal, the Kerr Rotation, and the Kerr Ellipticity, consult the theses of H. Feil, W. Zeper, and W. Van Drent listed in the bibliography.

2.7.4 Determining Kerr Rotation and Kerr Effect from Intensity Measurement

To facilitate the calculation of θ_K and ε_K , the ratio of $I(p)/I(0)$ and $I(2p)/I(0)$ is taken.

$$\frac{I(p)}{I(0)} = A \frac{J_1(\delta_0) \Delta R / R}{1 + J_0(\delta_0) \sin(\Delta\theta + 2\phi)} \quad \frac{I(2p)}{I(0)} = A \frac{2J_2(\delta_0) \sin(\Delta\theta + 2\phi)}{1 + J_0(\delta_0) \sin(\Delta\theta + 2\phi)}$$

A correction constant A must also be introduced as a factor to account for the laser beam's interaction with the system components. During a measurement, angle ϕ of the analyzer is set to zero. Also, the phase shift $\Delta\theta \ll 1$. The above equations simplify to

$$\frac{I(p)}{I(0)} = AJ_1(\delta_0) \frac{\Delta R}{R} \quad \frac{I(2p)}{I(0)} = AJ_2(\delta_0) 2\Delta\theta$$

Substituting in the equations for Kerr rotation and Kerr ellipticity, and then solving for θ_K and ϵ_K , results in

$$\theta_K = \frac{1}{-AJ_2(\delta_0)} \frac{I(2p)}{I(0)} \quad \epsilon_K = \frac{1}{4AJ_1(\delta_0)} \frac{I(p)}{I(0)}$$

Once the correction constant A for the system is determined, the LIA can be used to measure the intensity ratios, and the Kerr rotation and Kerr ellipticity can be calculated. For a more detailed description of this method, consult the thesis of W. Van Drent listed in the bibliography.

2.7.5 Choosing the retardation angle δ_0

Below is a graph of the first three Bessel functions. This graph will be used to determine the best retardation angle for the PEM. There are two main considerations in choosing a retardation angle. The $I(p)$ and $I(2p)$ signals need to be maximized, and any dependence that $I(0)$ has on the Kerr Effect needs to be minimized or eliminated. The graph indicates the first maximums for $J_1(x)$ and $J_2(x)$ and the first zero for $J_0(x)$. When

$J_0(x) = \text{zero}$, $I(0)$ has no dependence on the Kerr Effect. $J_0(x)$ occurs at $x = 2.4$ radians.

Note that when $x = 2.4$ radians, $J_1(x)$ and $J_2(x)$, while not at maximum, are still relatively large. Therefore, a retardation angle of 2.4 radians was chosen for the PEM.

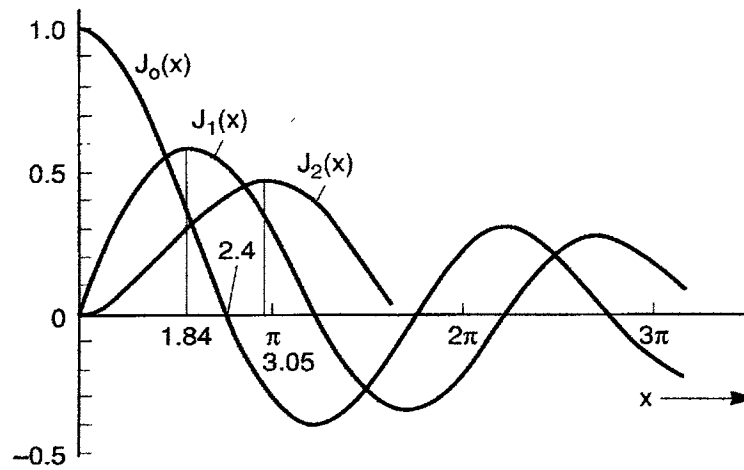


Figure 2.9 The First Three Bessel Functions¹²

CHAPTER 3

SAPPHIRE BALL CELL

3.1 The Diamond Anvil Cell

To determine if high pressure causes a shift in the Kerr peak towards shorter wavelengths, magneto-optical samples are placed in a Sapphire Ball Cell (SBC), which puts the sample under high pressure (~ 2 GPa) while still allowing measurement of the Kerr Effect. The SBC is a variant of the better-known Diamond Anvil Cell (DAC). Mao and Bell primarily developed the DAC, in its present form, at the National Bureau of Standards during the 1970's. It was developed out of a desire to make x-ray diffraction and spectroscopic studies of materials under high pressure¹⁴

The design of the DAC is relatively simple (see Figure 3.1). Two brilliant cut gem quality diamonds are placed in opposition with their flat sides facing each other. A small hole is then drilled through a metal gasket. The hole serves as the sample chamber. The sample chamber is filled with a pressure-transmitting medium (liquid or gas), the sample and a ruby crystal. The fluorescence of the ruby is used as a gauge to measure the pressure in the chamber. The gasket is placed and centered between the two diamond anvils. A hardened backing support is placed behind the two diamond anvils, and some sort of thrusting mechanism pushes the two anvils towards each other. As the volume of the sample chamber decreases, pressure-transmitting medium compresses the sample. The DAC can generally create up to 50 GPa of pressure. The two transparent diamonds allow x-ray diffraction, spectroscopy and other optical measurements of the sample.¹⁴

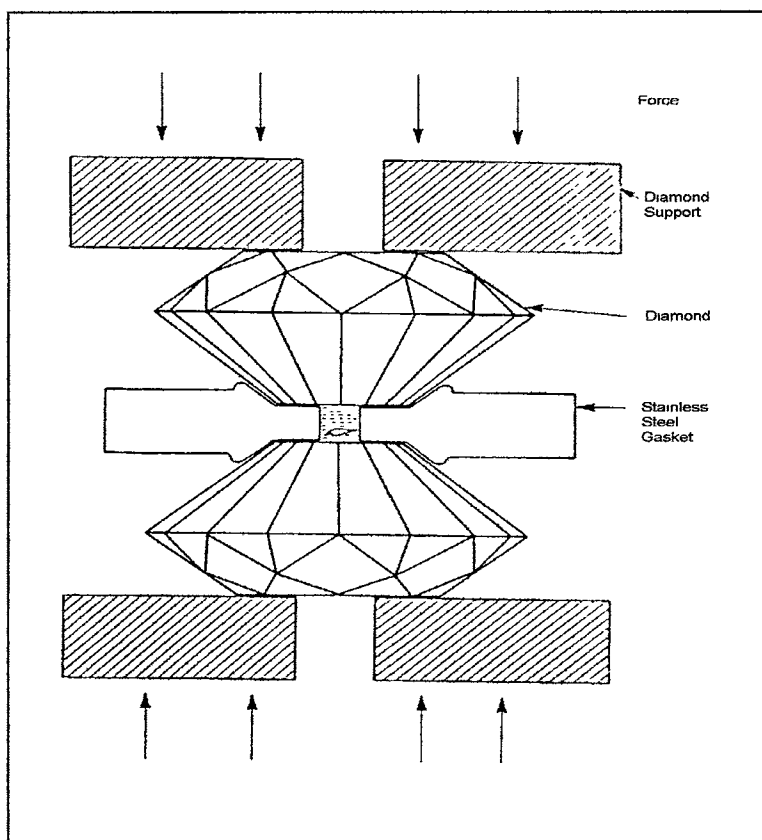


Figure 3.1 Diamond Anvil Cell¹⁴

The SBC works on the same principle as the DAC. The diamond anvils are replaced with the two sapphire spheres (Al_2O_3). A beryllium copper (BeCu) gasket is used, and the support and thrusting mechanism is integrated into the sapphire ball holders. Beryllium copper is a potentially hazardous material. The safety precautions detailed in Section 3 should be followed whenever working with BeCu. Four screws in the sapphire ball holders turn to move the sapphire balls towards each other to create the pressure.

A sapphire ball cell (SBC) creates isotropic pressures of up to two GPa in a small sample chamber ($< 1 \text{ mm}^3$).¹⁵ This pressure level is significantly smaller than that attainable in a DAC. However, a pressure level of two GPa is sufficient to measure any

shift in the Kerr peak. Cost is the primary advantage that the SBC has over the DAC. During the course of normal use, it is not unusual for a diamond anvil or a sapphire sphere to crack or shatter. Diamond anvils generally cost about \$1500, while sapphire balls only cost about \$10.

In addition, the SBC is generally simpler to build and operate. The four screws that provide the thrusting power are very straightforward to use. The SBC is bigger than the DAC. The sample chamber for a DAC is generally less than 0.2 mm. The sample chamber for the SBC is 0.5-0.9 mm. This difference in scale is important. With the SBC, it is possible to prepare and manipulate the sample and sample chamber with relative ease, using a tweezers, for example. The DAC requires equipment that is more sophisticated in order to accomplish the same tasks. Finally, the larger size of both the sample chamber and the sample make it easier to align the laser with the sample.

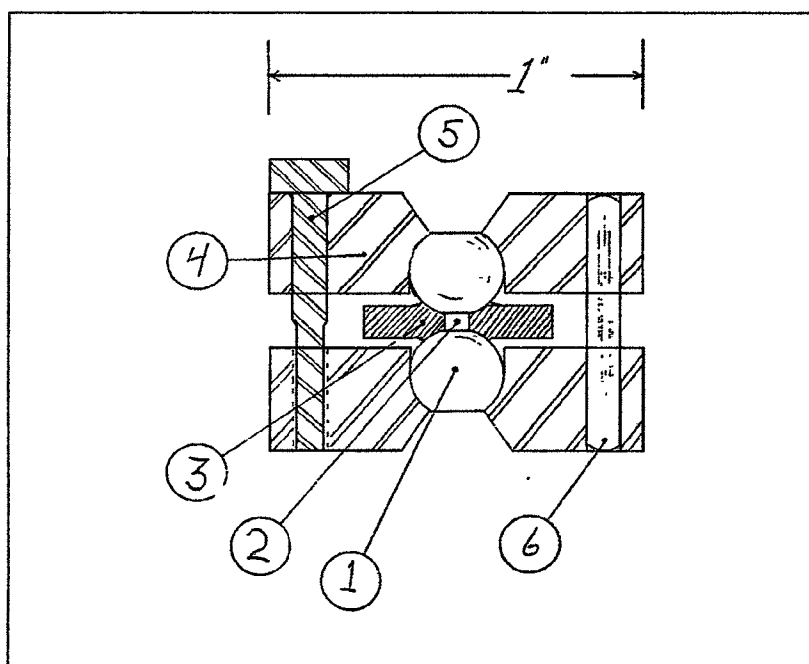


Figure 3.2 Basic Schematic of the SBC¹⁵

As shown in Figure 3.2, the SBC has five parts, which include

- two brass sapphire sphere holders (4)
- two sapphire balls (1)
- one Be-Cu gasket (3)

In addition, four non-magnetic screws (5) are used to slowly bring the two holders together and compress the sample chamber (2). The bottom sapphire sphere holder has two stainless steel pins to secure the Be-Cu gasket. Each sapphire ball holder has two dowels and two dowel holes (6). By inserting the dowels of one holder into the dowel holes of the other holder, the sapphire balls are brought into alignment with, and opposition to, each other. The SBC used at Southwest Texas State is based on the design of W. B. Daniels, et. al.¹⁵, and was built by ID Machine shop in San Marcos, TX (see Appendix A).

3.2 Beryllium Copper Gasket

The gasket is made from ¼ hard tempered beryllium copper (BeCu), 0.02 in. (0.5 mm) thick, manufactured by NGK Metals (see Appendix A). The BeCu is in the form of a roll of strip metal 1.5 in. (3.81 cm) wide. BeCu is a hard, non-magnetic metal that can still be compressed by the sapphire spheres. Each gasket is just over one centimeter long; so three gaskets can be cut from along the width of the BeCu coil strip.

Warning! BeCu dust is a **carcinogen!** Always wear a breath mask and eye goggles when cutting or drilling BeCu. Also coat the BeCu with oil to catch the BeCu dust.

The stainless steel holding pins on the SBC are 9.52 mm apart center-to-center. Two holes must be drilled through the gasket at this distance apart. Only the Enco drill press in the machine shop is precise enough to drill the holes at the right distance. A center punch is used to pre-indent the holes. These pre-indentations serve as a guide for the much thinner and easy-to-bend drill bit. A size 67 drill bit will cut the holes to the proper size. The drill bits should be coated with oil to minimize drill bit breakage. A size 67 drill bit is quite frail and easily breaks, so several spare drill bits should be kept on hand.

After the holes have been drilled, the gasket can be cut out of the strip. The gasket should be about 1.1 cm long and 5 mm wide. The Dremel tool, with its cutting circle attachment, can cut the gasket out of the strip. The gasket should fit snugly over the holding pins on the SBC.

Assuming that the gasket is a good fit, it is now possible to determine where the sample chamber should be cut in the gasket. The SBC should be assembled with the new gasket on the holding pins. The two halves of the SBC can be pressed together with sufficient force to cause the sapphire spheres to dent the gasket. Remove the gasket from the SBC. The dent in the gasket serves as a guide for making the sample chamber hole. The sample chamber should be between 0.5 mm and 0.9 mm across and can be made using a drill bit or a punch. After the sample chamber is made, putting the gasket back into the SBC and looking through one of the sapphire spheres can verify the position of the sample chamber. An image of the sample chamber should be visible and centered through the sapphire sphere.

3.3 The Sapphire Spheres

3.3.1 Crystal Structure and the Polarization

The sapphire spheres are each 0.635 cm (1/4 inch) in diameter, and transparent to visible light (see Appendix A). The laser beam must travel through the sapphire sphere to reach the sample, and then must travel back out of the sphere to get to the detector. As the beam travels through the sapphire sphere, its polarization may be affected by the crystal structure of the sapphire. This change in polarization must be eliminated to ensure accurate measurement of the sample's Kerr Effect.

Sapphire has a hexagonal close packed (hcp) crystal structure. The structure has a

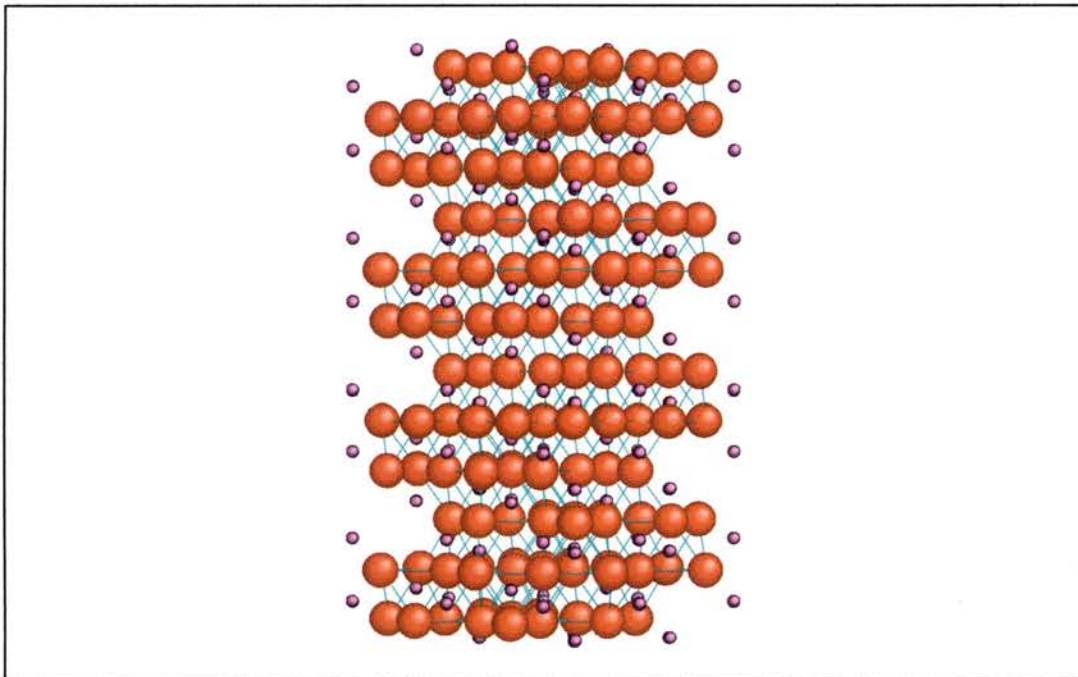


Figure 3.3a Sapphire (Al_2O_3) – C-axis Vertically Oriented

c-axis (or easy axis) along the (001) direction. If the propagation of light is along the c-axis, the crystal structure is equivalent for the x- and y-component of the laser beam.

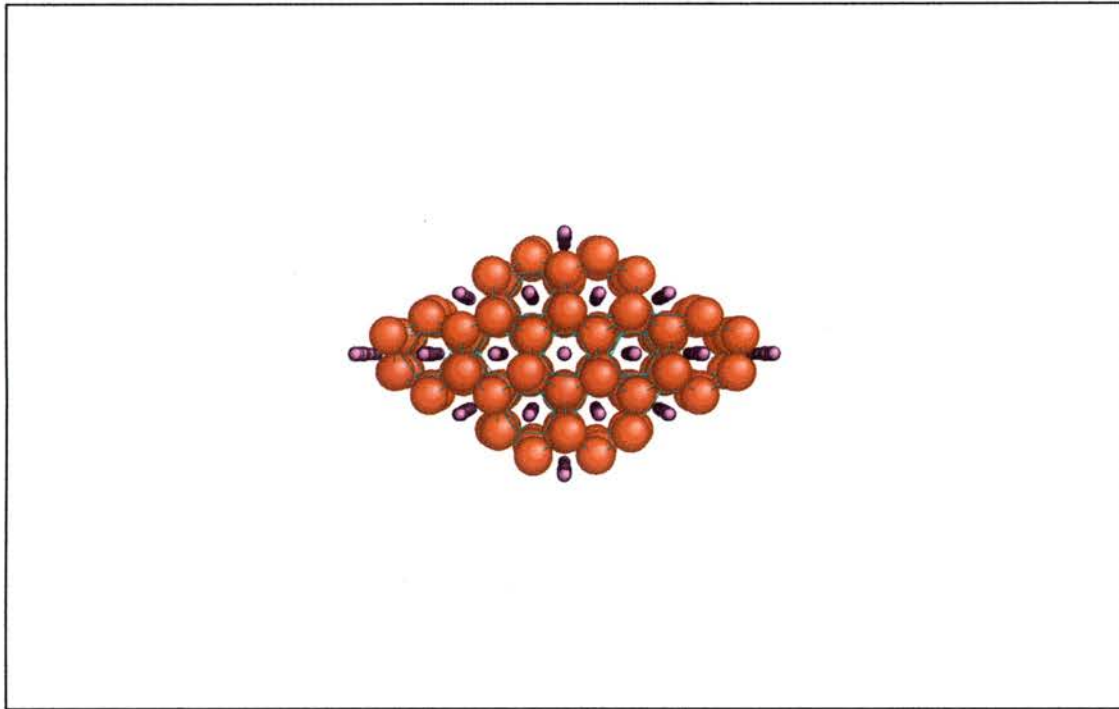


Figure 3.3b Sapphire (Al_2O_3) – Plane Perpendicular to C-axis

The complex refractive index will be the same for both components, and there will be no net change in the polarization. Figure 3.3 shows two views of sapphire's crystal structure. Each image was generated using CaRINE.

3.3.2 Determining the C-Axis of the Sapphire Sphere

A laser, two polarizers, a screen, and a sapphire sphere are arranged on the optical table according to Figure 3.4. Before placing the sapphire sphere between the polarizers, the polarizers should be rotated until no laser light reaches the screen. The transmittance axes of the two polarizers are then ninety degrees to each other. The sapphire sphere is then placed in the beam between the points. The sphere should rest on a stand that will keep it in the laser beam while allowing the sphere to be freely rotated.

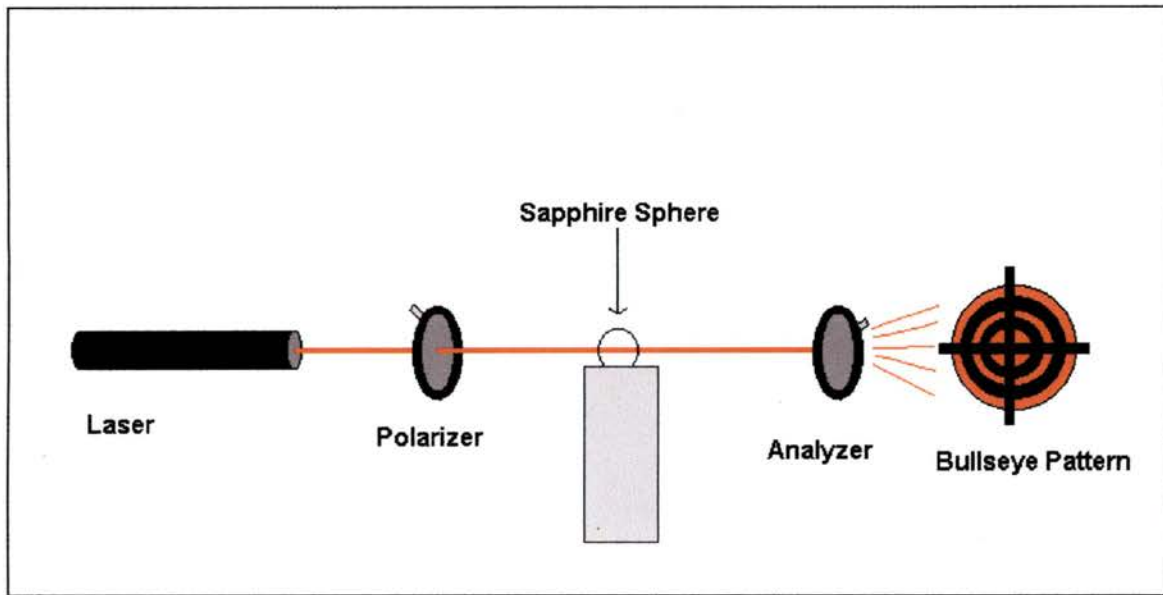


Figure 3.4 Determining the C-axis



Figure 3.5 Bulls Eye Pattern

The crystal structure of the sphere changes the polarization of the laser beam. An interference pattern should be visible on the screen. The sphere can be rotated with a Q-tip or a latex covered finger. When the “cross in a bulls eye” pattern appears, as in Figure

3.5, the laser is travelling through the c-axis. With the sphere in place, the c-axis can then be marked with a dark magic marker.

3.3.3 Polishing the Flats

3.3.3.1 The Necessity for Creating the Flats

The sapphire spheres must be flattened on opposite ends of the sphere along the c-axis. One of the flat sides will face the center hole of the sapphire sphere holder. This flat side is the “window flat”. The laser will enter and exit the SBC through this side. The other flat side, the “sample flat”, faces the sample chamber.

These flats have three functions. First, they permanently mark the c-axis of the sapphire sphere. In addition, when the laser is hitting the sample, the beam will be crossing only flat surfaces, both on incidence and reflection. This simplifies the description and calculation of the beam’s refraction and reflection at the air/sapphire and sapphire/sample chamber interfaces. Finally, the sample chamber flat will exert a uniform pressure throughout the sample chamber as the volume decreases.

3.3.3.2 The Window Flat

Creating the window flat is more complicated than creating the sample flat because the window flat is significantly larger. The window flat must be as large as the center hole in the sapphire sphere holder, which is 3.18 mm (1/8 inch). The best way to create the window flat is with a chemical mechanical polisher (CMP).



Figure 3.6 Chemical Mechanical Polisher

A Buehler Phoenix Beta CMP (Figure 3.6) was used to create the window flats on the sapphire spheres. The CMP is designed to polish thin films and comes with epoxy and accessories that allow the operator to create mounts for the thin film substrates. These epoxy mounts fit into the head of the CMP. Epoxy mounts can also be created to hold the sapphire spheres.

The epoxy comes as two separate ingredients (a liquid and a powder), which must be mixed together to form the hard epoxy. Several blue, hard rubber cups serve as molds to form the epoxy mount to the correct dimensions to fit the CMP head. Four thin, metal, circular plates were made to fit into the bottom of the blue cups. A 1/8 inch hole was drilled through the center of each plate. A 1/4 inch drill bit was then used to create a “sink” for the sapphire spheres to rest in.

The c-axis of the sapphire spheres should already be indicated by a mark. The spheres should be glued into the circular plates such that the c-axis mark is visible through the bottom (i.e., the c-axis should be perpendicular to the plate).

The CMP can polish four samples at a time; so four spheres and plates should be prepared at the same time. The plates, with sapphire spheres, rest snugly into the bottom of the blue cups.

Approximately 10 grams of the liquid component and 20 grams of the powder component will make two epoxy mounts. The two components should be measured separately in the disposable trays provided by Buehler. The Fisher Scientific Model A-160 digital scale was used to measure the desired masses.

Mixing the two components causes an exothermic reaction. Initially the mixture has the viscosity of syrup, but it will quickly harden. Therefore, the mixture should immediately be poured into the blue cups containing the sapphire spheres. The epoxy should completely cool and harden after 10-15 minutes.

It is relatively easy to remove the epoxy mount from the blue cup and to remove the metal plate from the bottom of the epoxy mount. The sapphire sphere should now be enclosed by the epoxy except for the c-axis end of the sphere, which should be sticking out of the bottom of the epoxy mount, as in Figure 3.7.



Figure 3.7 Epoxy Mount (~1 inch dia.) with Sapphire Sphere

The epoxy mounts can now be placed into the CMP head. The CMP should be set to 5 N of force at 200-rpm contra-motion. Water is a good slurry. Diamond lapping films, from Allied High Tech Products, Inc. (See Appendix A), of three different grits are used to polish the spheres. The epoxy mounts should be left in the CMP head when the diamond lapping films are changed.

Table 3.1 Polish Times of the Window Flats

First Polishing	15 microns	20 minutes
Second Polishing	1 micron	30 minutes
Third Polishing	0.1 micron	15 minutes

The exposed part of the sphere should now be flat and polished. Contact with the flats should be avoided in order to preserve their smoothness. The window flats should be specular to light, to help keep the laser beam crisp and clean. Acetone or some other dissolving fluid will soften the epoxy enough to dig the spheres out of the epoxy mount.

3.3.3.3 The Sample Flat

The sample flat is relatively small. It only needs to be larger than the sample chamber. As a result, it is easy to make compared to the window flats. The sample flats should be made after the window flats are made. A sapphire sphere should be glued into each SBC sphere holder, with the window flats properly oriented. A rectangular strip of metal about 0.5 cm wide and 5 cm long should be cut out of a sheet of metal. The metal strip needs to be hard and unbendable. It is important that the two sides of the metal strip are flat and parallel to each other.

A drop of diamond grit paste from Wendt Dunnington (see Appendix A) should be placed on both sides of the metal strip. With a toothpick, isocut fluid from Buehler (see Appendix A) should be mixed in with the paste. The metal strip should be placed between the two spheres of the assembled SBC. The diamond grit and the metal strip should be in contact with both of the spheres. The metal strip should be moved back and forth, with even strokes, between the two spheres, for approximately ten minutes, as in Figure 3.8. This should be done three times, using diamond paste with a grit of 30 microns, then 1 micron, and then 0.1 micron.

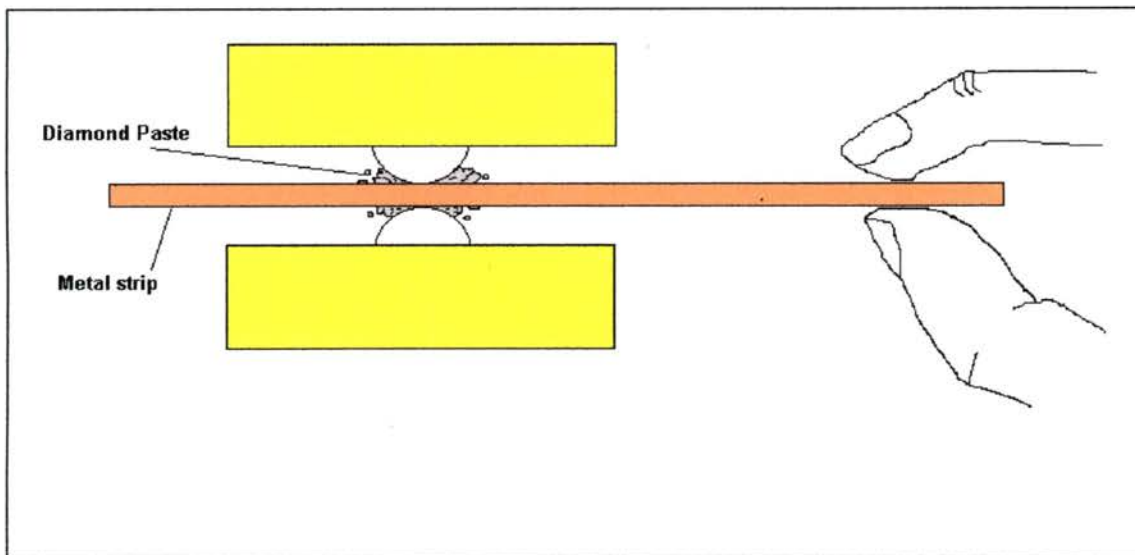


Figure 3.8 Creating the Sample Flats

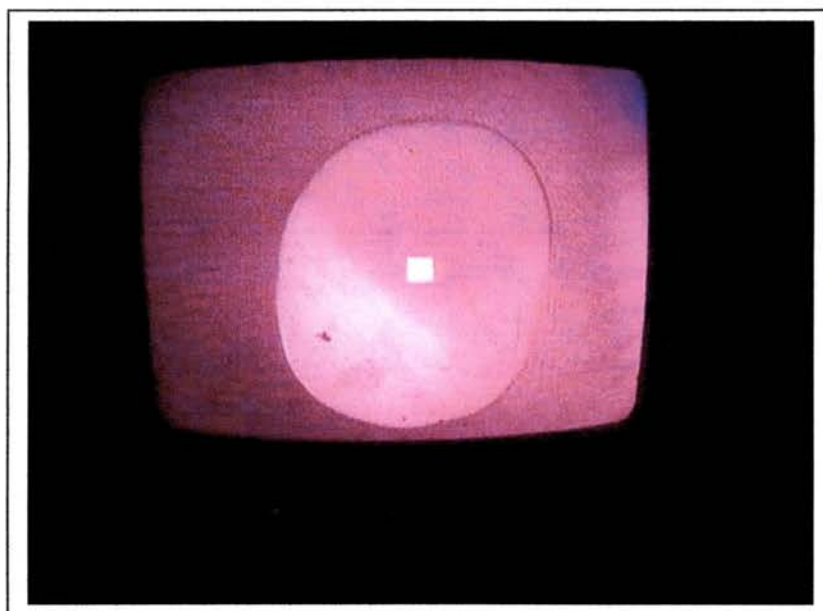


Figure 3.9 Sample Flat Under 5X Microscope

This procedure should create two sample flats, one on each sphere that are equal in size and smoothness, and are parallel to each other. The sample flats should be approximately 1 mm across. Figure 3.9 shows a sample flat under a 5X microscope. The

white square is a focusing mechanism. The spheres should not come into contact with each other. Sudden contact between the spheres can cause cracks and fissures.

3.4 Sample Preparation

The small volume of the sample chamber ($< 0.5 \text{ mm}^3$) necessitates that the sample also have a small volume. Therefore, most samples will come from thin films of magneto-optical materials grown on substrates. A section of the thin film must be removed from the substrate to serve as a sample. A fine razor blade is sufficient to cut the thin film. It may be of interest to note if the film tends to curl when removed from the substrate. This could indicate that the film was stressed. Due to the small size of the sample (0.5 mm x 0.5 mm), a magnifying glass is very helpful in cutting a sample.

Tweezers and needles are generally too big to handle the sample. An ultra thin wire taped to a wooden Q-tip is fine enough to manipulate the sample. Again, a magnifying lens or low power microscope is useful in this situation. Ultra thin wire is used to place the sample in the sample chamber, and the sample chamber is filled with the pressure-transmitting fluid. The SBC should then be carefully reassembled. Backlighting the SBC and looking through one of the sapphire spheres can verify the position of the sample in the sample chamber. The sample should be visible inside the sample chamber.

3.5 Generating and Measuring Pressure

3.5.1 The Pressure in the Cell

The four non-magnetic screws pass through the bottom sapphire sphere holder to screw into the top sapphire sphere holder. The screws should be tightened until they are

just hand-tight. At this point the sapphire spheres are just resting against the gasket. In the sample chamber, the distance between the two spheres is 0.5 mm (the thickness of the gasket).

If the screws continue to be tightened, the two spheres will press into the gasket, and the volume of the sample chamber will decrease. One complete rotation of a screw will move the screw 0.72 mm. A 1/3 rotation on each screw will bring the two spheres to within approximately 0.25 mm of each other. The sample chamber will be approximately 1/2 of its original volume.

If the pressure-transmitting medium is a gas, then the ideal gas law governs the change in pressure in the sample chamber.

$$\Delta P = \frac{NRT}{\Delta V}$$

If $\Delta V = 1/2 V_0$, then $\Delta P = 2P_0$. Pressure has an inverse linear relationship to volume.

If the pressure-transmitting medium is a fluid, then the change in pressure is governed by

$$\Delta P = -B \left(\frac{\Delta V}{V_0} \right)$$

B is the bulk modulus of the pressure-transmitting medium. This equation is valid for both liquids and solids. For example, the bulk modulus for water is $2.2 \times 10^9 \text{ N/m}^2$. If water is used as the pressure transmitting medium, and the volume of the sample chamber is decreased by 1/2, then the change in pressure is

$$\Delta P = -(2.2 * 10^9 \text{ N/m}^2) * \left(-\frac{1}{2}\right) = 1.1 * 10^9 \text{ N/m}^2$$

This is about 10,000 atmospheres! For a sample made from steel ($B = 160 \times 10^9 \text{ N/m}^2$), the decrease in volume (and, therefore, lattice spacing) resulting from this change in pressure is given by

$$\frac{\Delta V}{V_0} = \frac{1.1 * 10^9 \text{ N/m}^2}{-160 * 10^9 \text{ N/m}^2} = 0.006875$$

This scale of change in the lattice spacing is necessary to measure any shift in the Kerr peak due to pressure. From literature, the most common pressure transmitting fluid for the DAC is an ethanol/methanol mixture.¹⁴ The bulk modulus of this mixture is slightly less than that for water, but, unlike water, this mixture remains a liquid at the high pressures in the SBC. The index of refraction for the ethanol/methanol mixture is approximately 1.34. For the SBC, it would be ideal if the index of refraction of the pressure transmitting fluid matched the sapphire sphere. This would eliminate any reflection or refraction at the sphere/sample chamber interface. SPI Supplies (see Appendix A) produces liquids of various indices of refraction for the fiber optic industry. A diomethane sulfur mixture with an index of refraction of 1.775 was purchased to use as a pressure-transmitting medium. It is still unknown if the diomethane sulfur mixture will remain a liquid under the high pressure in the SBC.

3.5.2 Ruby Crystals as a Pressure Indicator

Ruby crystals are placed in the sample chamber to use as a gauge to measure the pressure in the chamber. At room pressure, ruby fluoresces at 694.2 nm. This peak of



Figure 3.10 Optical Multichannel Analyzer (OMA)

fluorescence shifts by 0.36 nm per GPa increase in pressure.¹⁶ The shift in the wavelength can be measured with Princeton Applied Research's Optical Multi-channel Analyzer (OMA) in connection with a photodetector from Jarrell-Ash (see Figure 3.10). The SBC is placed in the Argon Ion laser writer. The sample chamber is then illuminated with 488 nm laser light, causing the ruby crystals in the sample chamber to fluoresce. A fiber optic cable carries the light from the fluorescing ruby to the Jarrell-Ash photodetector. Using the 600-lines/mm diffraction grating, the OMA is precise enough (0.2 nm of wavelength) to detect the shift in the fluorescent peak at 2-3 GPa. It may be necessary to cool the photodetector in order to reduce the noise level.

CHAPTER 4

MEASUREMENTS

4.1 Alignment of Beam with the Sapphire Ball Cell (SBC)

The height of the laser needs to be adjusted so that the laser beam is at the same height as the sample chamber. The beam expander attaches directly to the front of the laser. However, the internal surfaces of the beam expander may reflect the beam back into the laser. This will destabilize the intensity of the laser. The laser controller will start clicking if the intensity destabilizes. To correct this, the beam expander may need to be detached from the laser and placed on its own stand. The beam expander needs to be slightly off axis to the laser beam to prevent reflections from entering the laser cavity.

The mirror is on a tilting stage, which can be used to fine adjust the direction of the reflected beam. The reflected beam should travel through the center of the quarter-wave plate, the PEM and the focusing lens, and then pass between the magnet pole pieces (See Figure 2.1). Use the Ardel Kinematic base to place the SBC at the centerpoint between the magnet pole pieces. The micrometer base of the focusing lens can then be used to move the laser beam onto the window flat of the sapphire sphere.

4.2 Hitting the Sample with the Laser

4.2.1 The Backlit Projection Method

The shape and orientation of the sample in the sample chamber should be determined before the SBC is placed between the magnet poles. This can be done under a microscope or by looking through the sapphire spheres when the sample chamber is

backlit. This is necessary because it is impossible to directly observe the sample chamber when the SBC is between the magnet poles.

Some method other than direct observation must be used to determine when the laser is striking the sample. When the laser strikes the sample hole, the laser light will travel through the sample hole and exit the SBC through the other sapphire sphere. A plano-convex lens can be used to expand this light to get a good backlit projected image of the sample chamber on a screen. By adjusting the position of the beam, the shape of the sample chamber and the sample can be discerned. If the laser is in fact striking the sample chamber, then the shape of the backlit-projected image of the sample should match its true shape. If this is the case, the beam should then be adjusted to strike the sample. Figure 4.1 shows the backlit-projected image of the sample chamber on the left. On the right is a photograph of the sample chamber produced by placing a light directly behind the sample chamber

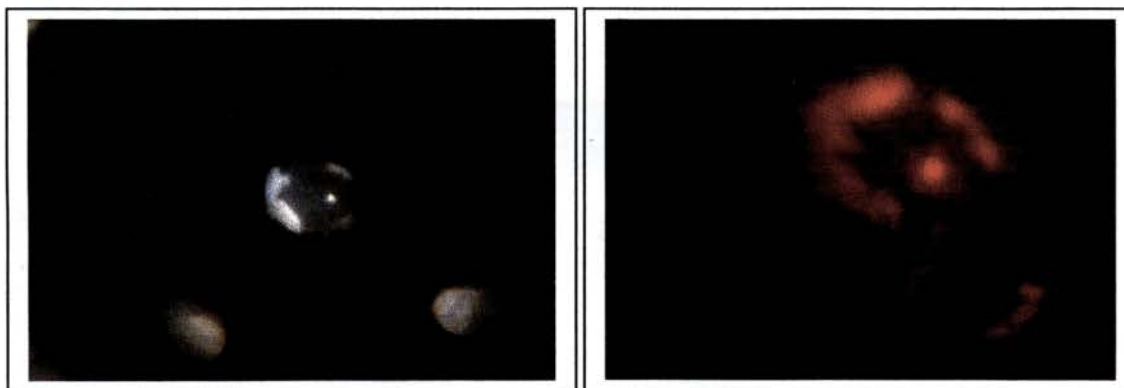


Figure 4.1 A Direct Image (Left) and Backlit Image (Right) of Sample

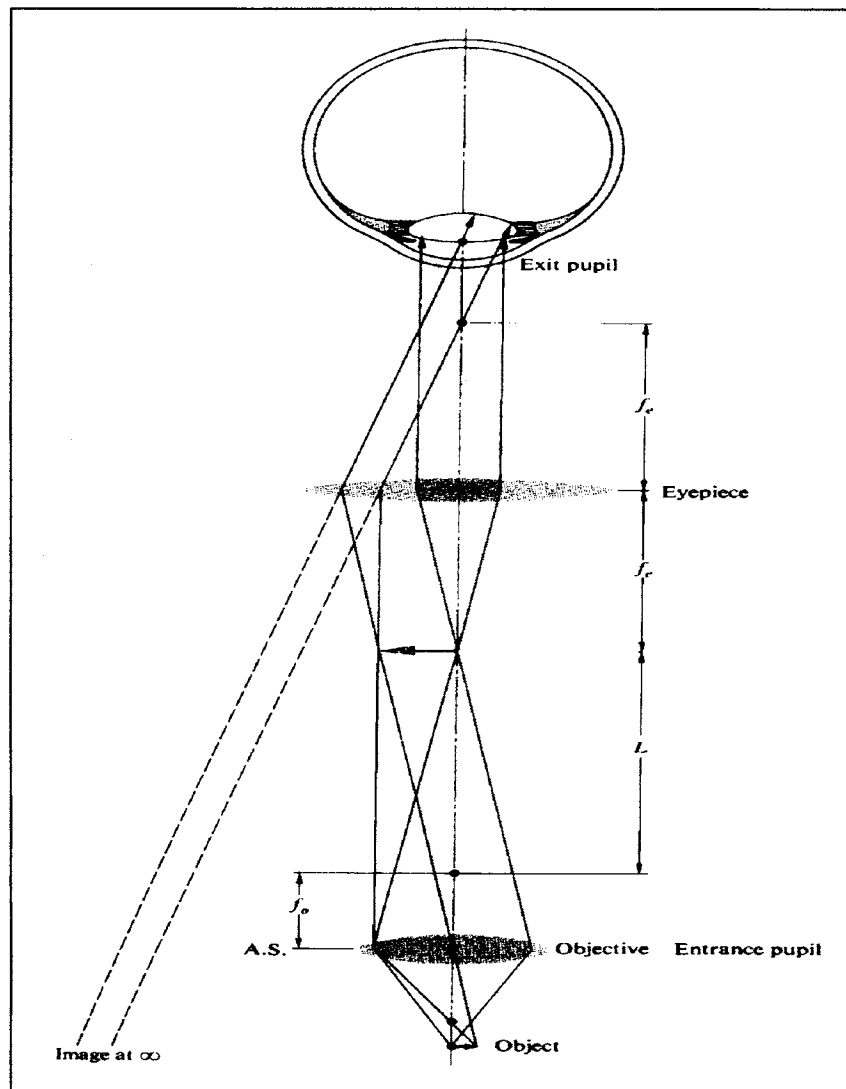


Figure 4.2 Simple Compound Microscope²

4.2.2 The Microscope

A mirror and two lenses were used to build a “microscope” to view the laser spot on the gasket. Figure 4.2 shows a diagram of a simple compound microscope.

The magnification power (MP) of the microscope is determined by

$$MP = \left(-\frac{L}{f_o} \right) \left(\frac{N.P.}{f_e} \right)$$

where f_o and f_e are the focal points of the objective lens and the eyepiece lens, respectively, and $N.P.$ is the standard near point of normal (20/20) human vision, which is

10 inches. The near point is the closest point on which the eye can focus. L is the distance from the second focal point of the objective lens to the first focal point of the eyepiece lens, called the *tube length*.² From the equation, we learn that the focal lengths of the two lenses should be minimized and the tube length should be maximized in order to increase magnification. From the rays shown in Figure 4.2, it can be seen that the maximum tube length L is determined by the diameter of the two lenses and the distance between the object and the focal point of the objective lens. The magnification of the image of the object increases as the object gets closer to the focal point. However, eventually the object gets so close to the focal point that the lenses are no longer large enough to resolve a clear image of the object. Therefore, to maximize the tube length the diameters of the two lenses should be large and the distance between the object and the objective lens' focal point should be minimal.

Two converging lenses and a small mirror are used in the Kerr measurement setup as a microscope to view the sample chamber. Because of the geometry of the setup, it is difficult and inconvenient to set up the lenses to directly view the sample chamber. Instead, a small mirror is used to reflect the image to the lenses. The mirror is oriented at a 45-degree angle to the SBC and placed between the incident laser beam and the reflected laser beam, as in Figure 4.3. In order to minimize both the focal length of the objective lens and the distance between the SBC and the lens' focal point, the overall distance between the SBC and the objective lens should be as short as possible. However, neither the mirror nor the objective lens can be allowed to block either the incident beam or the reflected beam.

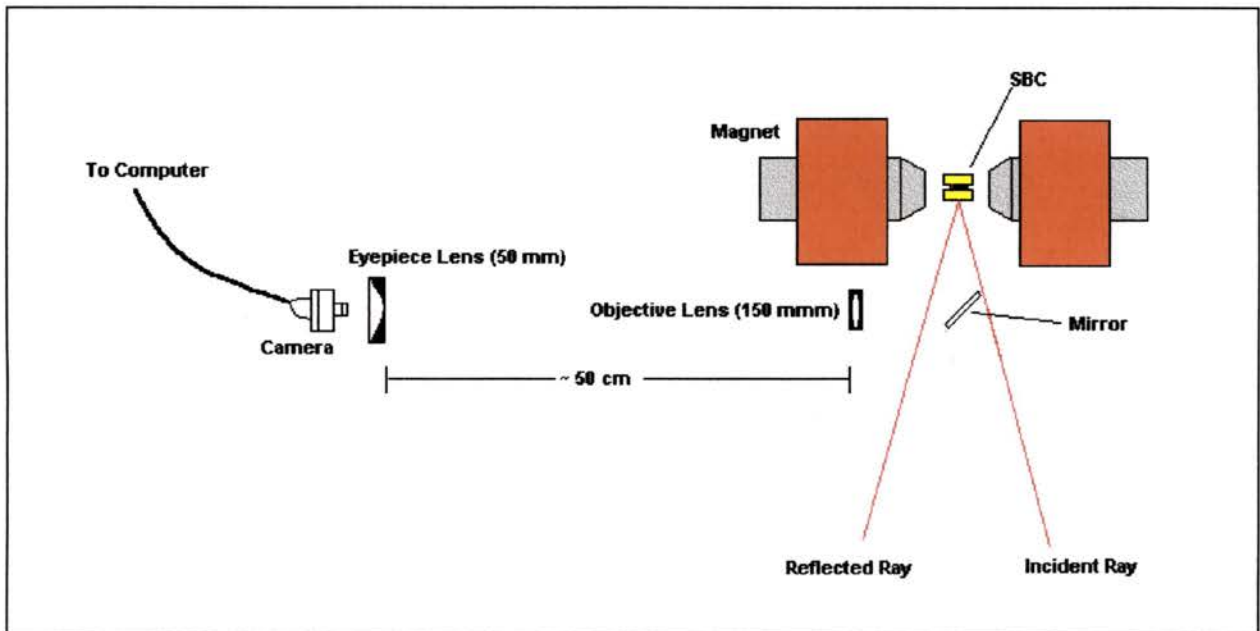


Figure 4.3 Microscope Setup

The mirror stand used in the Kerr measurement setup was approximately one inch across. This mirror allowed for a minimum focal length of approximately 150-mm for the objective lens. A lens with a shorter focal length would block one of the beams. Figure 4.3 shows the microscope setup. The 150-mm double convex lens was 1.5 inches in diameter. A two-inch diameter plano-convex lens with a focal length of 50 mm was used as the eyepiece lens. Approximately fifty centimeters separated the two lenses.

The image of the sample chamber can be observed at the eyepiece. It was found to be most convenient to place a video camera at the eyepiece and feed the image to a computer that had a video card installed. Wavewatcher TV-PCI was used to observe the video image. The reflected laser appears as a white spot on the gasket. The focusing lens can then be adjusted to bring the laser onto the sample chamber. The backlit-projected method can be used to confirm that the laser is striking the sample.

4.3 The Reflected Beam and the Signal at the Photodetector

The reflected beam will diverge. A fused silica lens should be used to converge the reflected light to the analyzer and photodetector. It is important that none of the light strikes the edge of either the analyzer's or the photodetector's aperture. If the reflected light strikes an edge, then some of the light is being blocked and is not reaching the photodetector. Vibration of the setup will cause changes in the intensity of the light that reaches the photodetector. This translates into noise in the intensity signal. Since the Kerr measurement setup measures changes in intensity, any noise in the intensity signal of the reflected light not caused by the Kerr Effect is unwanted. In addition, edges cause diffraction of the light, which is unwanted.

The reflected light causes current in the silicon photodiode photodetector. The voltmeter measures the voltage difference in the photodetector that is driving the current. This voltage is directly related to the intensity of the light. The photodetector is not designed to carry more than 3.5 Volts across it. If the reflected beam is generating more than 3.5 Volts, then the sensitivity of the photodetector must be adjusted downward. Conversely, if the reflected beam is generating significantly less than 3.5 Volts, then the sensitivity of the photodetector should be adjusted upwards. The voltage generated by the reflected beam should be maximized to the limitations of the photodetector.

The Kerr measurement setup is designed to measure the intensity of the horizontal component of the reflected light. Recall from Chapter 2, Section 7, that the $I(0)$ and $I(2p)$ signals are dependent on the analyzer angle ϕ . Ideally, for consistency of measurement, ϕ should always be set to zero. Then the intensity variation is solely dependent on the Kerr Effect. An analyzer angle of zero corresponds to the axis of transmission being

horizontal, parallel to the tabletop. Therefore, it is important that the analyzer completely blocks the vertical component of the light. When the vertical component of the light has been blocked, the intensity of the reflected beam at the photodetector will be at a minimum. Consequently, the voltage measured by the voltmeter will also be at a minimum. The analyzer should be manually rotated so that the axis of transmittance is horizontal. The analyzer has a micrometer on it so that the direction of the axis of transmittance can be finely adjusted. The micrometer can be used if the setscrew on the analyzer is tightened so that the analyzer can no longer be manually adjusted. When the ac-voltage as indicated on the LIA or scope is at a minimum, then the analyzer angle is zero and the detected light only contains the horizontal component. The minimum can also be determined by minimizing the Kerr signal on the oscilloscope.

4.4 Determining the Correction Constant A

From Chapter 2, Section 6, the Kerr Rotation(θ_k) and Kerr Ellipticity(ϵ_k) are given by

$$\theta_k = \frac{1}{-4AJ_2(\delta_0)} \frac{I(2p)}{I(p)}$$

$$\epsilon_k = \frac{1}{4AJ_1(\delta_0)} \frac{I(p)}{I(2p)}$$

The correction constant A must be calculated before a measurement can be taken. The correction constant is determined by rotating the analyzer from $\phi = -2$ degrees to $\phi = +2$ degrees in 0.5 degree increments and monitoring the $I(2p)/I(0)$ signal on the LIA. This ratio can be described by

$$\frac{I(2p)}{I(0)}(\phi) = 2AJ_2(\delta_0)\sin(2\phi - 2\phi_k)$$

or, by using the small angle approximation,

$$\frac{I(2p)}{I(0)}(\phi) = 4AJ_2(\delta_0)(\phi - \phi_k)$$

No magnetic field is applied while the correction constant is determined. Any remnant Kerr Rotation in the sample is defined as zero. Letting $A_{rot} = 4AJ_2(\delta_0)$, the above equation simplifies to

$$\frac{I(2p)}{I(0)} = A_{rot}\phi$$

A_{rot} is defined as the rotation correction constant. $I(2p)/I(0)$ is a linear function of the analyzer angle ϕ . The graph of the measured values of $I(2p)/I(0)$ versus ϕ should produce a linear curve with a slope equal to A_{rot} .³¹ Once A_{rot} has been determined from the graph, the ellipticity correction constant (A_{ell}) can be calculated using the following relationship.

$$A_{rot} \frac{-J_1(\delta_0)}{4J_2(\delta_0)} = A_{ell}$$

For a more detailed explanation of the theory and method for determining the correction constant, see the thesis of W. Van Drent listed in the bibliography.

4.5 Taking a Measurement

The software that controls the electronic components and takes a measurement is called “Kerr Tracer” and is located on the “Sparks” computer in the optical characterization lab. The Kerr Tracer program was written using LabView by Harsha Abeywickrema and Wilhelmus Geerts at Southwest Texas State University. A shortcut to the program should be on the desktop. All of the electronic components should be powered up before the program is opened. As indicated on the first screen, the program can measure either the Kerr Rotation or the Kerr Ellipticity. Before a measurement can be taken, a file name must be chosen for the measurement data and typed into the “Output File” field. The file name should be descriptive so that any one who reads it knows what sample was measured and when the measurement was taken. The desired maximum field strength (up to 5000 gauss) should put into the “Magnetic Field Amplitude” field. The “# Data Points” field indicates the number of intensity measurements that the computer makes every quarter-cycle of the hysteresis curve. For example, if the operator inputs “10” into this field, the computer will take forty data points, with ten points on each “leg” of the measurement, as indicated below.

0 field to max. positive field	10 points
max. positive field to 0	10 points
0 field to max. negative field	10 points
max. negative field to 0 field	10 points

The “# samples/point” field indicates how many measurements of the intensity the computer makes at a given field strength. The average value of the intensity measurements is then used to generate the data point. The “# cycles” field indicates the number of hysteresis curves that will be taken in this measurement. Once the desired values are typed into these fields, a measurement can be taken by pressing the “Start Measurement” button. The computer quickly goes through one cycle of the magnet without taking any measurements. The field goes to maximum positive, then maximum negative, and then back maximum positive. This magnetizes the sample before any measurements are taken, ensuring a normal hysteresis curve. The computer then starts to take data points. Each measurement generates a graph showing voltage versus applied field, which is displayed on the screen.

The computer also generates a data file that contains the field strength, the AC voltage at each field strength, and the DC voltage at each field strength. From Chapter 2, Section 6, the DC voltage corresponds to the $I(0)$ intensity, and the AC voltage corresponds to the $I(p)$ intensity (for Kerr Ellipticity), or to the $I(2p)$ intensity (for Kerr Rotation). To analyze the data, the file must be saved onto a floppy disk and transported to a computer that has Excel on it.

4.6 Initial Measurements

Great difficulty was encountered in obtaining and measuring a reflected beam from a sample in the SBC. Before any measurements were attempted using the SBC, several measurements were taken of a BiYG thin film grown on a silicon substrate. The following hysteresis curve (Figure 4.4) was generated when measuring the Kerr Rotation.

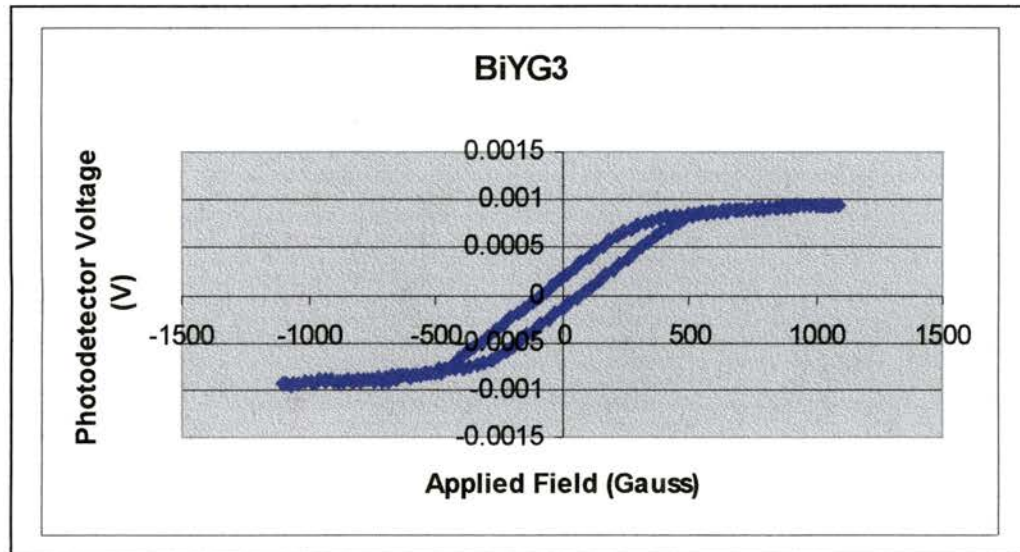


Figure 4.4 Hysteresis Curve for BiYG Film

These measurements confirmed that the optical table setup could measure the Kerr Effect. Measurements were then taken of the BiYG film with the incident and reflected laser beam travelling through one of the sapphire spheres. These measurements generated only garbage. The flats on the sapphire spheres may not be sufficiently polished and smooth. In the future, spheres that already have flats should be handled carefully to ensure that the flats remain smooth and uncontaminated. The angle between the laser beam and the c-axis of the sapphire crystal structure may be large enough to introduce an unwanted polarization. Attempts were made to take polar Kerr measurements with the laser beam travelling through a hole in one of the pole pieces of the magnet. In this setup, the laser beam has an angle of incidence of about one degree. However, the small angular aperture afforded by the hole in the pole piece (~ 2 degrees) made it virtually impossible to get the reflected beam back to the photodetector. This issue has yet to be resolved.

CHAPTER 5

CONCLUSIONS

5.1 Concluding Remarks

Many digital data storage devices utilize the Magneto-Optical Kerr Effect (MOKE) to read/write data. Currently, these devices use red laser light because most common magneto-optical materials show a more pronounced Kerr Effect for red light than for shorter wavelengths. The wavelength at which a material shows the greatest Kerr Effect is called the Kerr peak. Theoretical calculations suggest that if a material is placed under high pressure, the Kerr peak will shift to shorter wavelengths. Shorter wavelength lasers can then be used to read/write data, which, according to the Rayleigh criteria, would allow an increase in data density.

The Kerr measurement setup in the Optical Characterization Lab uses an intensity-stabilized laser to measure the Kerr Effect for magnetized samples. The setup generates hysteresis curves that show Kerr rotation or Kerr Ellipticity as a function of the magnetic field applied to the sample.

The sapphire ball cell (SBC) is a high-pressure cell that allows direct optical measurements of the sample in the pressure cell. The SBC is then placed into the Kerr measurement setup so that the Kerr Effect for the pressurized sample can be measured.

Techniques were created for aligning the equipment and aiming the laser at the sample. A procedure for polishing the sapphire spheres and creating the gaskets was also developed. The behavior of the incident and reflected light as it traveled through the SBC was studied. A method was developed, using ruby fluorescence, for measuring the

sample chamber pressure. Criteria for the optimal pressure transmitting fluid were developed.

5.2 Recommendations for Future Research

In order for the Kerr Effect to be measured, the reflected beam must exit the SBC. The angular aperture for the laser to enter and exit the SBC is small (~ 20 degrees). This makes the orientation of the sample in the sample chamber critical. In order for the reflected beam to exit the SBC, the surface of the sample must be parallel to the surface of the gasket. The angle of incidence will then be about ten degrees, and the laser will reflect at an angle that allows it to exit. If the sample surface is not parallel to the gasket, then the angle of incidence will be significantly greater than ten degrees, and the reflected laser beam will not exit the SBC. Some technique must be developed for keeping the sample at the proper orientation.

The Kerr measurement setup in the Optical Characterization Lab can currently measure the Kerr Effect at only one wavelength (632.8 nm). Even if the Kerr Effect at this wavelength is shown to decrease with pressure, that is not enough to indicate that there has been a blue shift in the Kerr peak. Measurements at shorter wavelengths need to be taken to confirm that the Kerr Effect at those wavelengths increases with pressure.

The Physics Department at Southwest Texas has purchased a Micro Electric Discharge Machining (EDM) System from Hylozoic Products for the Optical Characterization lab. EDM systems are used to cut and machine metal, and can be used on almost any metal. Material is removed from the metal by localized melting. The Micro EDM System was purchased for its versatility and efficacy in drilling and machining small parts. Both samples and sample chamber holes can be cut to precise

dimensions. With EDM, the edges of the sample chamber will be sharp and free from burrs in comparison to a hole drilled by a normal bit. The Micro EDM System should make the creation of the gaskets and the samples easier, while increasing the quality of both.

APPENDIX A

List of Suppliers and Manufacturers

Item	Provider	Contact Info	Address
Photoelastic Modulator	Hinds Instruments	1(800) 688-4463 www.hindspem.com	3175 NW Aloclek Dr Hillsboro, OR 97124
Laser	Melles Griot Laser Group	(760) 438-2131 102722.1210@compuserve.com	2251 Rutherford Rd Carlsbad, CA 92008
CMP, Isocut Fluid	Buehler, Ltd.	(847) 295-6500	41 Waukegan Rd Lake Bluff, IL 60044
Sapphire Spheres	Swiss Jewel Company	(215) 925-2867 www.swiss-jewel.com	Lafayette Building Philadelphia, PA 19106
Diamond Paste	Precision Surfaces International	(800) 843-0950 www.psidragon.com	Houston, TX
Diamond Lapping Films	Allied High Tech Products, Inc.	(800) 675-1118	2376 E. Pacifica Pl. Rancho Dominguez, CA 90220
Beryllium Copper	NGK Metals Corp.	(610) 921-5000	529 W. Rincon St. Corona, CA 91720
Diomethane Sulfur	SPI Supplies	www.2spi.com	West Chester, PA 19381
Sapphire Ball Cell	ID Machine Shop	353-8272	703 Uhland Rd San Marcos, TX 78666

BIBLIOGRAPHY

- ¹P.M. Oppeneer, "Ab initio investigation of microscopic enhancement factors in tuning the magneto-optical Kerr effect," *Physics B – Condensed Matter* 88 (1992): 311.
- ²Eugene Hecht, *Optics*, Third Edition, New York: Addison Wesley Longman, Inc., 1998.
- ³Hans Feil, "Magneto-optical Kerr effect. The relation between optical, transport and electronic properties in magnetic compounds.," Ph.D. diss., University of Groningen, 1987.
- ⁴David Jiles, *Introduction to Magnetism and Magnetic Materials*, New York: Chapman and Hall, 1991.
- ⁵Mark H. Kryder, "Magneto-Optical Storage Materials," presented at the Annual Review Materials Science 1993, Carnegie Mellon University, Pittsburgh, Pennsylvania (1993) (unpublished).
- ⁶Melles Griot, "Stabilized HeNe Laser System," Melles Griot Laser Group, Carlsbad, CA, (1994)
- ⁷Oriel Instruments, "The Book of Photon Tools," Oriel Instruments, Stratford, CT, (1999)
- ⁸Hinds Instruments, Inc., "PEM-90 Photoelastic Modulator Systems User Manual," Hinds Instruments, Inc., Hillsboro, OR, (1996).
- ⁹Stanford Research Systems, Inc., "Model SR830 DSP Lock-In Amplifier," Stanford Research Systems, Inc., Sunnyvale, CA, (1993).
- ¹⁰William Van Drent, "CoNi/Pt Multilayers for Magneto-Optical Recording." Ph.D. diss., University of Twente, 1995.

- ¹¹Wilhelmus Geerts, "A set-up for measuring magneto-optical Kerr hysteresis curves at high fields and low temperature," submitted to *Rev. Sci. Instrum.*, 2001.
- ¹²W. Bas Zeper, "Magneto-optical recording media based on Co/Pt multilayers." Ph.D. diss., University of Twente, 1991.
- ¹³Thornton, Stephen T., and Rex, Andrew, *Modern Physics for Scientists and Engineers*, Ft. Worth: Saunders College Publishing, 1993.
- ¹⁴A. Jayaraman, "Ultrahigh pressures," *Review of Scientific Instruments* 57, no. 6 (June 1986): 1014.
- ¹⁵W. B. Daniels, "Simple Sapphire Ball Cell for High Pressure Studies in the Ultraviolet," presented at the XIII AIRAPT Conference, Bangalore, India (1991).
- ¹⁶R.C.G. Naber, "Report on Diamond Anvil Cell research project '98-'99," University of Groningen, 1998, 9; available from <http://www.chem.rug.nl/ssc/projects/dac.html>; Internet.

VITA

Brian Christopher Donehew was born in Denver , Colorado, on January 13, 1969, the son of Gerald Ray and Edith Marie Donehew. He graduated from James Madison High School in San Antonio, Texas, and then earned a B.B.A. in Accounting from Texas A & M University in College Station, Texas. After spending a couple of years as an auditor in industry, he returned to school and earned a B.S. in Math and a B.A. in Physics from the University of Texas at San Antonio. In January 1999, he began working on his Masters of Science in Physics at Southwest Texas State University in San Marcos, Texas.

His work in the Optical Characterization Lab at Southwest Texas State has resulted in the following papers and presentations some of which are awaiting publication.

- 1) Wilhelmus Geerts, Brian Donehew, Vaughan Williams, Thomas Schmiedel, A set-up for measuring magneto-optical Kerr hysteresis curves at high fields and low temperature, Rev. Sci. Instrum.
- 2) F Hellman, W Geerts, B Donehew, "Magneto-optic Measurements of amorphous-Gd-Si Alloys," Annual Report, National High Magnetic Field Laboratory, 2001.
- 3) "The Magneto-Optical Kerr Effect under High Pressure," Joint Fall Meeting of the Texas Sections of the APS, AAPT, and SPS; Texas Christian University, October 2001

- 4) "The Effect of High Stress on the Kerr Effect for Metals," Texas Academy of Sciences Meeting, March 2001, Southwest Texas State University
- 5) "High Pressure and the Kerr Effect for Magneto-Optical Materials", Southwest Texas State University Summer Research Program 2000

Permanent Address: 4506 Buckmoor
 San Antonio, TX 78217

This thesis was typed by Brian Christopher Donehew